CHAPTER 4

DEVELOPMENT OF TLD DESIGN PROCEDURES

Design guidelines for TLDs based upon the numerical models discussed in Chapter 3 are described. The design guidelines are based upon the effectiveness measure defined as the reduction in peak structural displacement. Because the guidelines are based upon the interaction of the TLD with the structural system, this interaction model will be presented before loading-specific investigations are discussed.

4.1 Interaction of a TLD with a SDOF structure

Because the TLD is attached to a SDOF structure, the dynamic structural responses to the external forces are based upon its inherent damping and the damping forces generated by the TLD. In Section 4.1.1, this nonlinearly coupled system is formulated. Numerical solution schemes for the coupled system in time domain are proposed.

4.1.1 Time history numerical solution schemes

Figure 4.1(a) shows the system of a SDOF structure equipped with a TLD. The hydrodynamic force generated by water sloshing motion acts as a resisting force (or, damping force) to the external force. The coupled system is treated as a SDOF system subjected to the total external force which is sum of the damping force, F_d and the external force, F_e. The equation of motion of the coupled system is expressed as

$$m_s\ddot{x}_s + c_s\dot{x}_s + k_s x_s = F_e + F_d \tag{4.1}$$

where m_s, c_s and k_s are mass, damping constant and stiffness constant and x_s is structural displacement, respectively. To determine F_d in the equation, the water sloshing motion is simulated using the RCM model at each time step. The damping forces, i.e., the hydrodynamic forces due to the water sloshing, are calculated from the wave height at the

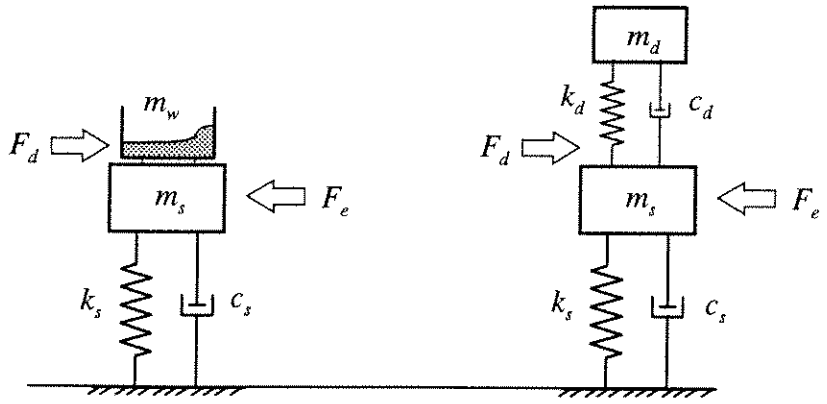

(a) TLD as RCM model (b) TLD as NSD Model

Figure 4.1 A SDOF structure with a TLD

end walls using Equation (2.15). Equation (4.1) is now solved analytically for each time step as described in Appendix D. The solution procedure is schematically illustrated in Figure 4.2.

Figure 4.1 (b) shows the equivalent system in which the TLD is characterized by the NSD model. The coupled system is treated as a traditional 2DOF system. The equation of motion is written as

$$\begin{bmatrix} m_d & 0 \\ 0 & m_s \end{bmatrix} \begin{Bmatrix} \ddot{x}_d \\ \ddot{x}_s \end{Bmatrix} + \begin{bmatrix} c_d & -c_d \\ -c_d & c_d + c_s \end{bmatrix} \begin{Bmatrix} \dot{x}_d \\ \dot{x}_s \end{Bmatrix} + \begin{bmatrix} k_d & -k_d \\ -k_d & k_d + k_s \end{bmatrix} \begin{Bmatrix} x_d \\ x_s \end{Bmatrix} = \begin{Bmatrix} 0 \\ F_e \end{Bmatrix} \tag{4.2}$$

in which m, c, k and x are the mass, damping constant, stiffness constant and relative displacement of the structure, respectively. The subscripts d and s indicate the damper and structure, respectively. The quantities, m_s, m_d, c_s and k_s are given constants. The external forcing function F_e is approximated to be a constant at each time step of the numerical solving procedure. The damping constant c_d and the stiffness constant k_d of the NSD model are determined by Equations (3.9) and (3.10), respectively.

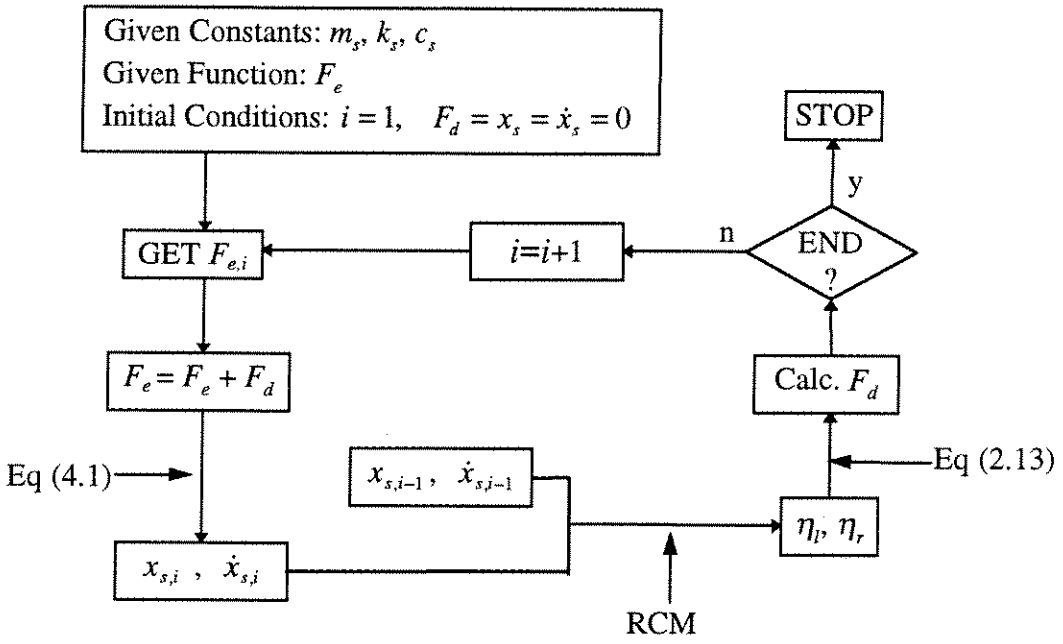

Figure 4.2 A numerical solution scheme for the responses of a SDOF structure coupled with a TLD. The TLD is simulated using the RCM model.

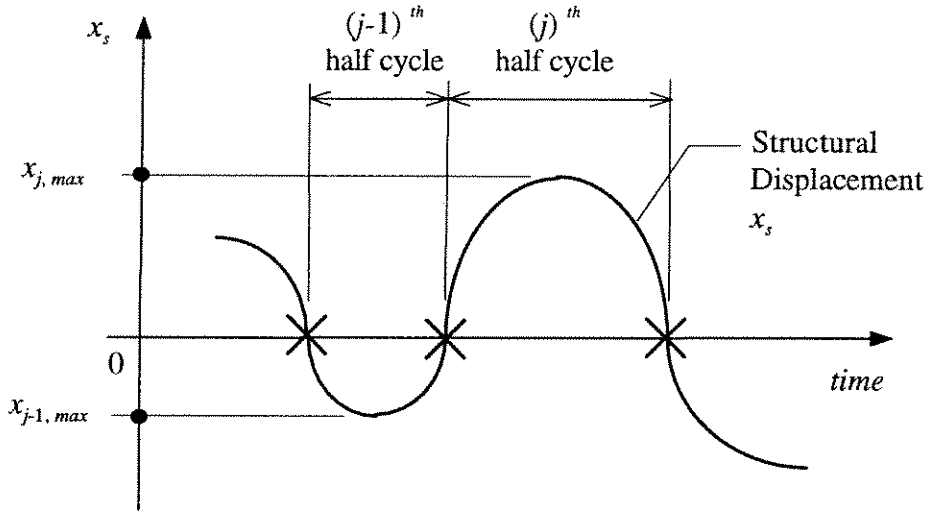

Figure 4.3 An arbitrary time history structural displacement.

Figure 4.3 shows an arbitrary sample time history structural displacement to illustrate how to determine the excitation amplitude A in Equations (3.9) and (3.10). Each time the structural displacement curve, x_s, crosses the horizontal time axis, the peak structural displacement, $x_{j-1,max}$ during the previous $(j\text{-}1)^{th}$ half cycle is sought. The absolute value of $x_{j-1,max}$ is assumed as the excitation amplitude A_j in Equations (3.9) and (3.10) during the next (j^{th}) half cycle to calculate c_d and k_d. The system stiffness and the damping matrices are reformulated with new values of c_d and k_d at this time step. Equation (4.2) is then solved using the Runge-Kutta method. The numerical solution procedure is illustrated in Figure 4.4.

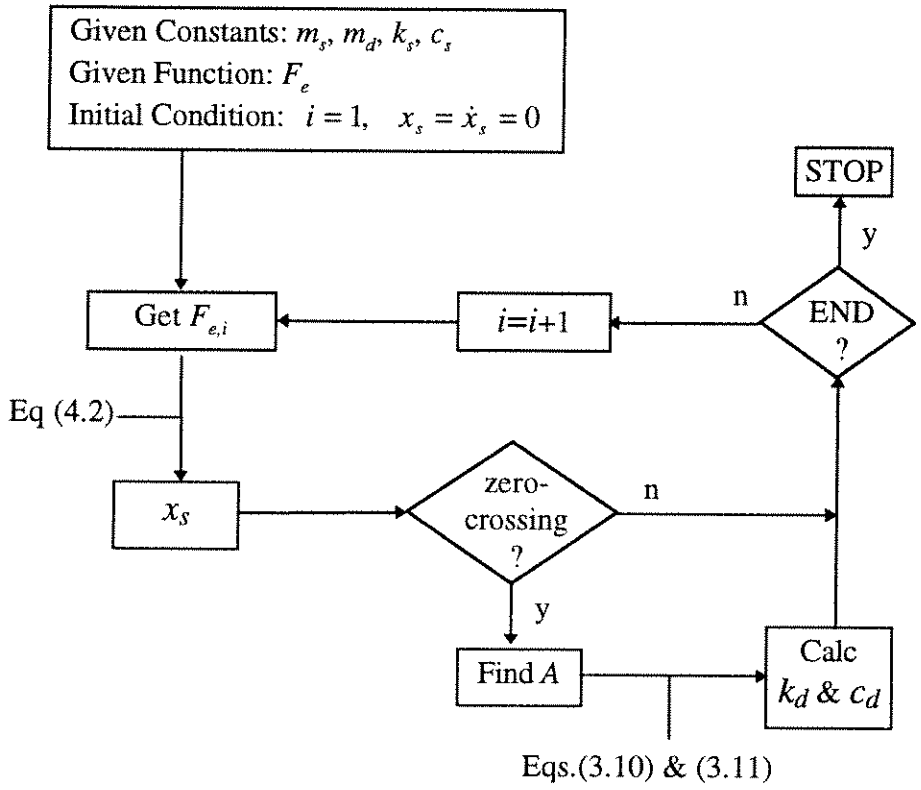

Figure 4.4 A numerical solution scheme for the responses of a SDOF structure coupled with a TLD. The TLD is characterized by the NSD model

4.1.2 Evaluation of the NSD model and the RCM model

It was shown in Figure 3.7 that the RCM model predicts accurately the energy dissipation capacity of the TLD in the region of weak wave breaking. It was also found, however, that the RCM model is not capable of predicting the energy dissipation capacity of the TLD in the strong wave breaking region. This limitation of the RCM model is verified through case studies in this section.

Consider the SDOF structural systems coupled with a TLD as shown in Figure 4.1. The properties of the selected systems are described in Table 4.1. In the first two cases, the tank size and the excitation amplitudes and frequencies fall into the range of the shaking table experimental investigations. The excitation amplitude for Case 1 was determined such that it falls into the region of weak wave breaking, i.e., A/L less than 0.03. Case 2 is for the same system as Case 1 but was subjected to stronger excitation which induces strong wave breaking in the TLD, i.e., A/L greater than 0.03. The tank size and the excitation amplitudes and frequencies for Case 3 fall beyond the range of shaking table experimental cases in order to evaluate the effectiveness of the NSD model in this range.

First, dynamic responses of the selected system for Case 1 under various excitation

Table 4.1 Data for case studies

Case	Structure		TLD				Exc.Amp(*1)
ID	f_s	ζ_s	L	h	f_w	μ	$x_{0,max}$
1	0.458 Hz	0.7 %	590 mm	30 mm	0.458 Hz	1.0 %	50 mm
2	0.458 Hz	0.7 %	590 mm	30 mm	0.458 Hz	1.0 %	100 mm
3	0.180 Hz	0.7 %	2300 mm	70 mm	0.180 Hz	1.0 %	200 mm

(*1) The magnitude of the harmonic forcing function is adjusted such that the maximum structural displacement without the TLD becomes these values at steady-state.

frequencies were obtained by solving Equations (4.1) and (4.2) using the RCM and the NSD models, respectively. Figure 4.5 presents the time history structural responses for several excitation frequency ratios, β = 0.95, 0.99, 1.00 and 1.10. The results from the RCM and the NSD analyses at each excitation frequency are plotted together for comparison. The maximum structural displacements in the entire time duration and at steady-state are presented in the plots. The results from the two analyses are in close agreement in terms of both the shape and magnitude of the time history of the structural displacements.

Figure 4.6 shows the time histories of the damping and the stiffness hardening ratios of the NSD model for the cases as in Figure 4.5. These two parameters are recalculated at every zero-crossing time step using Equations (3.9) and (3.10) as explained in the previous section. It is noted that the values of κ for all four excitation frequency cases are approximately constant at 1.05 regardless of the structural excitation amplitudes. This behavior occurs because the structural vibration amplitudes for all four frequency cases fall into the region of weak wave breaking, i.e., A/L < 0.03 in which the values of κ changes slowly as shown in Figure 3.3.

Figure 4.7 presents the comparison of the results from both analyses in terms of the maximum structural displacements at sweep excitation frequencies. The maximum structural displacements at steady-state are plotted in Figure 4.7 (a). The two results are in close agreement. It is observed that the TLD reduces the maximum structural displacements at steady-state by approximately 70 %, i.e., from 50 mm for the structure without TLD to approximately 15 mm with TLD. The maximum structural displacements in the entire time duration are plotted in Figure 4.7 (b). The two results show close agreement.

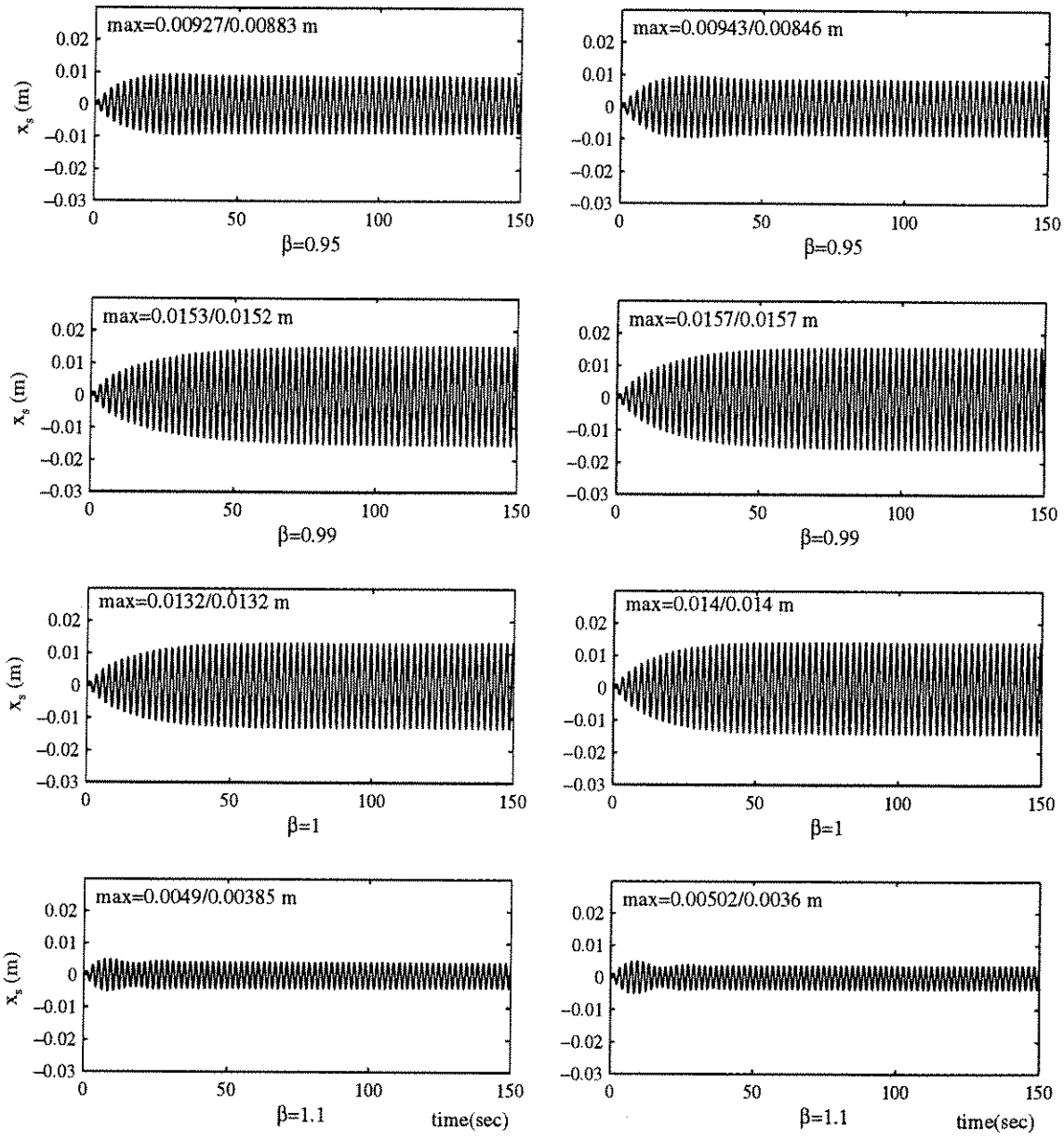

(a) RCM model (b) NSD model

Figure 4.5 Sample time history responses of the SDOF structure coupled with a TLD (Case 1). The TLD is characterized by the RCM and the NSD models, respectively. The excitation amplitude is in the region of weak wave breaking.

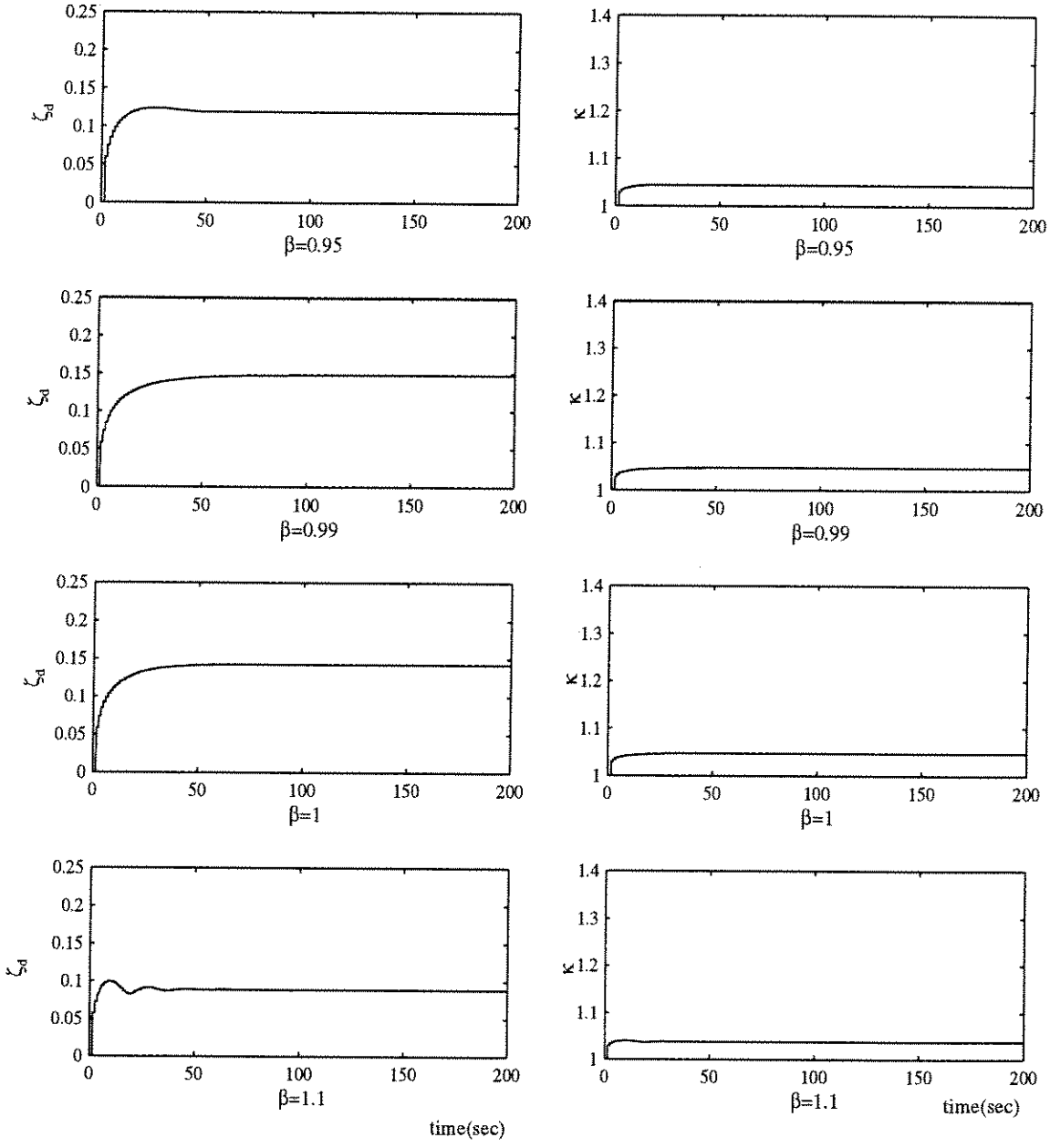

(a) Damping ratio (b) Stiffness hardening ratio

Figure 4.6 Sample time histories of the NSD model properties for the TLD for the same cases as Figure 4.5.

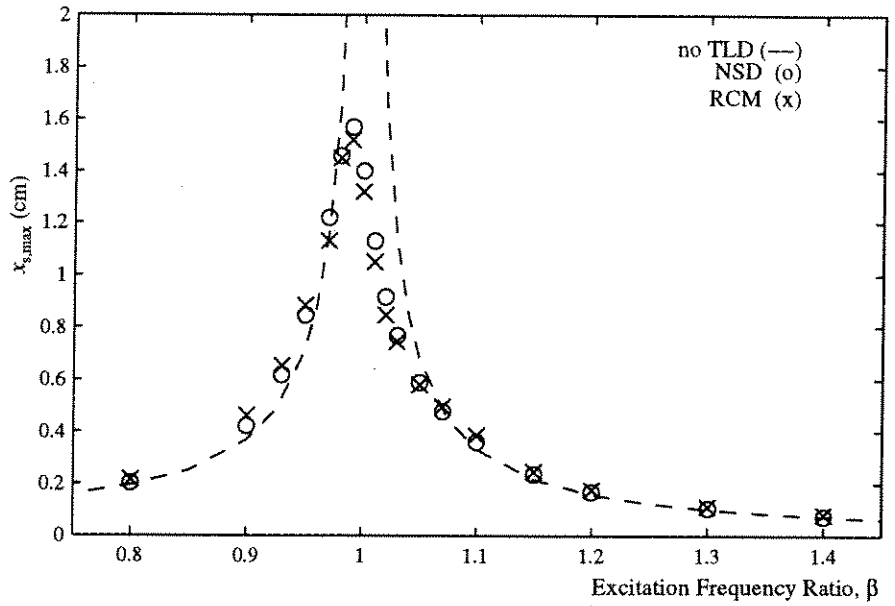

(a) Maximum structural displacement at steady state

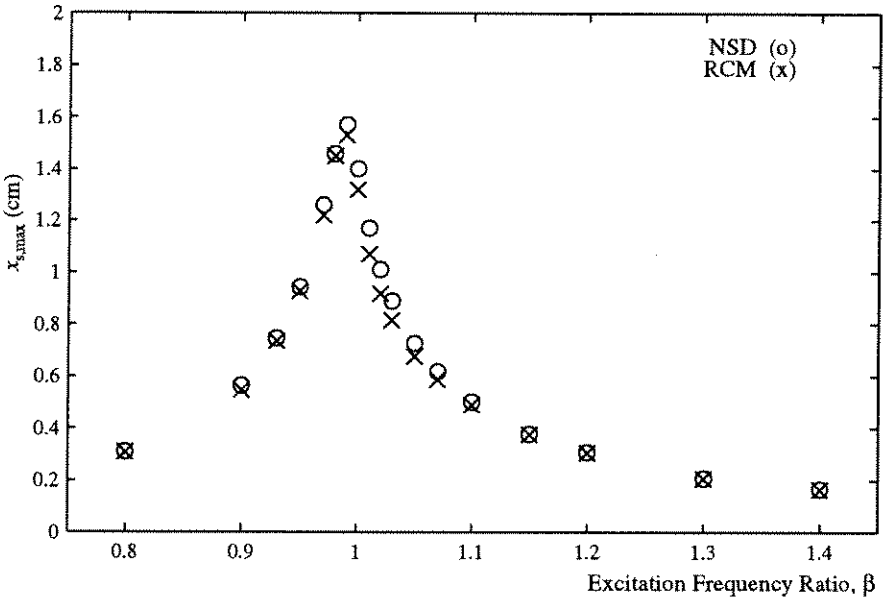

(b) Maximum structural displacement over entire period

Figure 4.7 The maximum displacements of the structure coupled with a TLD at sweep excitation frequencies. The TLD is characterized by the RCM and the NSD models, respectively. The excitation amplitude is in the region of weak wave breaking.

Next, the system for Case 2 was analyzed using two models in the same manner. The excitation amplitude in this case falls into the strong wave breaking region, i.e., A/L > 0.03, near the resonance frequency. As noted previously in Chaper 3, the RCM model cannot predict the TLD energy dissipation capacity accurately in this excitation range. The time history responses of the structure for Case 2 are presented in Figure 4.8 for several excitation frequencies, β = 0.95, 0.99, 1.00 and 1.10. The results from both analyses are plotted together for comparison. The results at excitation frequency ratios β = 0.95 and 1.10 are in close agreement. However, at β = 0.99 and 1.00 which are near resonance frequency, the structural displacement becomes larger and the values of the parameter A/L fall into the region of strong wave breaking, i.e., A/L is greater than 0.03. In this region, the RCM model has not predicted the behavior of the TLD accurately. The TLD develops stronger nonlinear behavior than predicted by the RCM model. Consequently, the TLD tuning is farther from the linear natural frequency and the structural natural frequency; therefore, it demonstrates less effectiveness.

Because the values of the NSD model parameters were derived based on the empirical results, the validity of the NSD model beyond the experimental range must be investigated. Case 3 was designed for this purpose. The selected structural natural frequency f_s = 0.18 Hz and the length of the TLD L = 2300 mm are outside of the range of the shaking table experimental cases. The water depth was determined such that the TLD is tuned to the structural natural frequency. The designated excitation amplitude $x_{0,max}$ = 270 mm was selected such that the steady-state structural motions for all excitation frequencies fell into the region of weak wave breaking. In this excitation region, the RCM model predicts the TLD behavior accurately. Numerical analyses were conducted using two models in the same manner as Case 1 and 2. The results are plotted in Figure 4.9. The results from the NSD model analyses demonstrate close agreement with those from the RCM model analyses for all excitation frequency cases. This result implies that the NSD model is valid for the conditions beyond those used for the derivation. In summary;

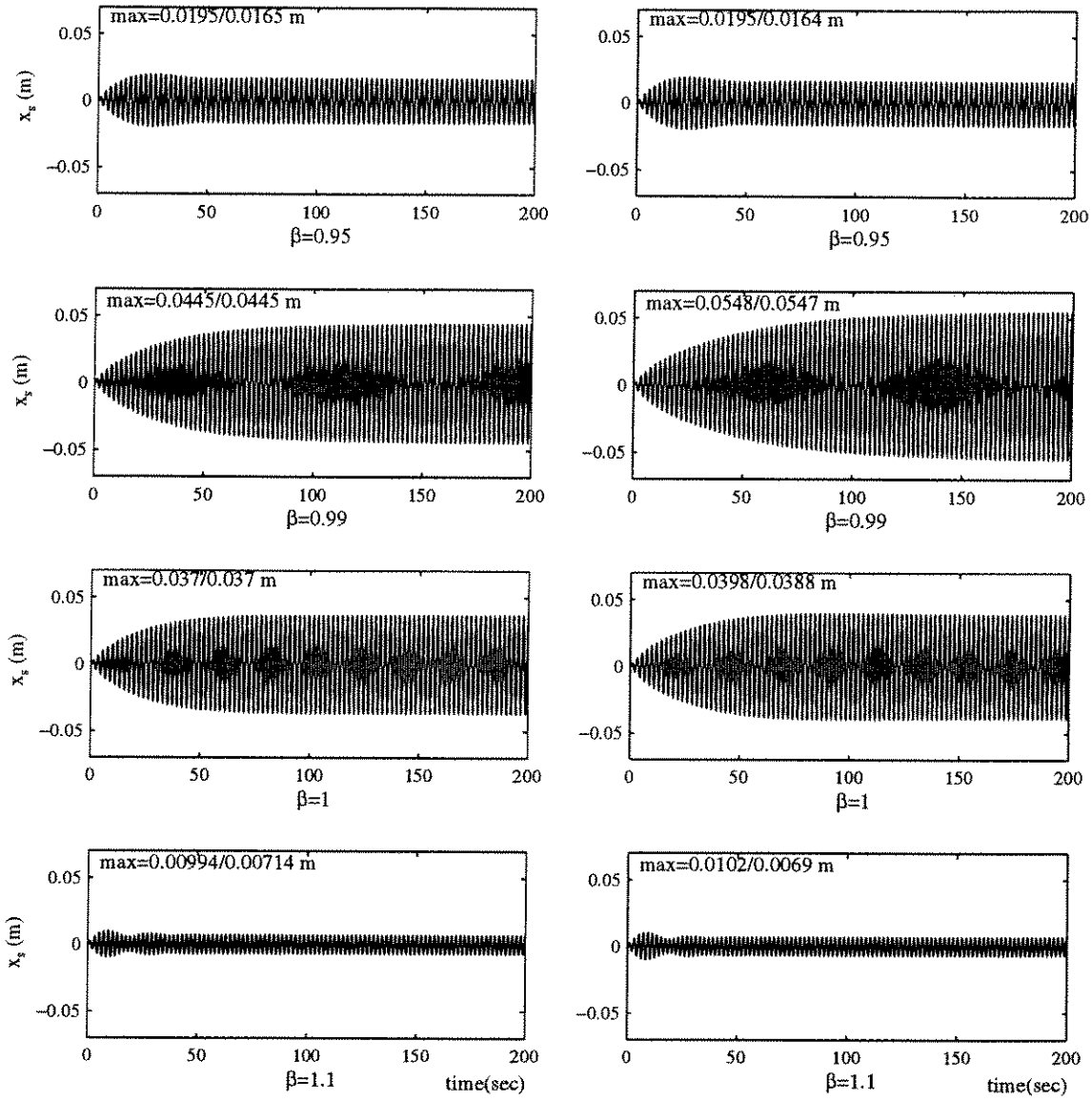

(a) RCM model (b) NSD model

Figure 4.8 Sample time history responses of the SDOF structure coupled with a TLD (Case 2). The TLD is characterized by the RCM and the NSD models, respectively. The excitation amplitude near resonance falls into the region of strong wave breaking.

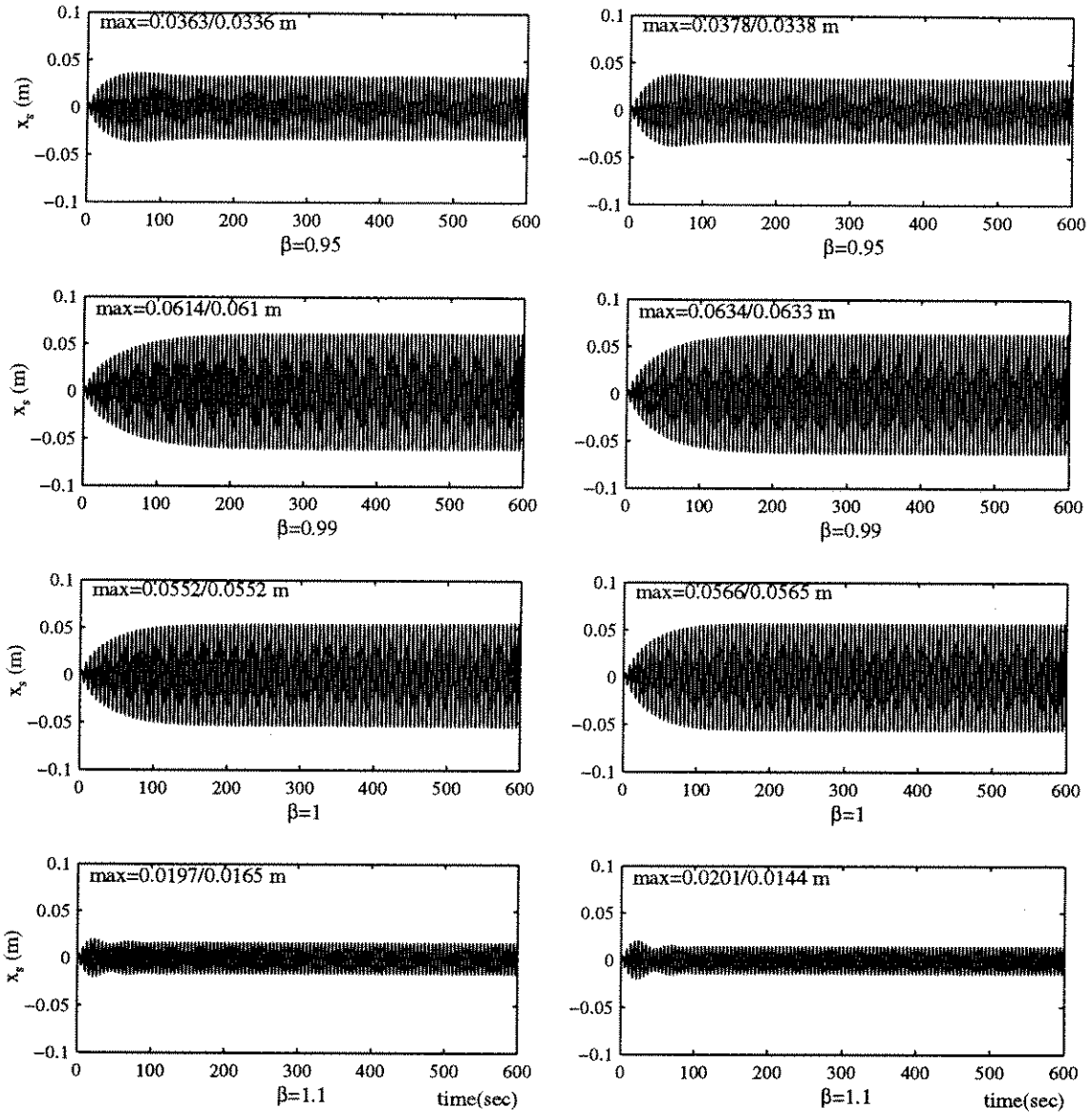

(a) RCM model (b) NSD model

Figure 4.9 Sample time history responses of the SDOF structure coupled with a TLD (Case 3). The TLD is characterized by the RCM and the NSD models, respectively. The selected system is in the condition beyond the experimental cases.

- The NSD model and the RCM model predict the TLD performance accurately in the excitation region of weak wave breaking.
- The RCM model does not adequately capture strong wave breaking.
- The NSD model which has been calibrated from the limited experimental investigation was shown to be valid for certain conditions which are beyond the limited experimental cases.

4.2 TLD performance and design procedure for harmonic excitations

In this section, the performance of TLDs coupled with a lightly damped SDOF structure is investigated for harmonic excitation. A frequency response analysis method coupled with an iteration procedure to solve the nonlinear system is proposed. The effectiveness of the TLD is defined as the reduction of the maximum displacement of the structure. The influence of the TLD nonlinearity on its effectiveness is evaluated. A simple TLD design procedure incorporating nonlinearity is proposed.

4.2.1 Frequency response analysis

A SDOF structural system equipped with a TLD can be modeled as a two-degree-of-freedom system by using the NSD model for the TLD as shown in Figure 4.10. The properties of the NSD model (k_d and c_d) are functions of the peak amplitude of the structural motion as described in Equations (3.9) and (3.10). As the structure is subjected to a harmonic excitation, the peak amplitude of the structural motion becomes a constant at steady-state. The properties of the NSD model (k_d and c_d), therefore, become constant at steady-state. Consequently, the TLD behaves like a linear system at steady-state. Therefore, the peak displacement of the structure at steady-state can be calculated by[1]

$$x_0 = \frac{F_0}{k_s} \frac{1}{\sqrt{RE^2 + IM^2}}, \tag{4.3}$$

[1] See Appendix B for detailed solution procedure

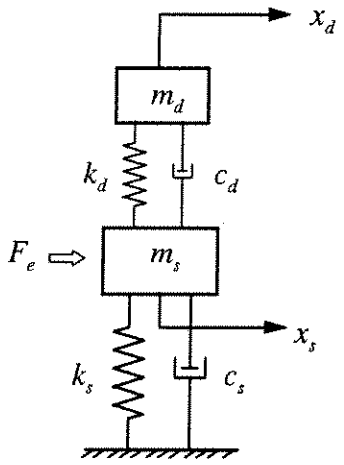

Figure 4.10 A SDOF structure equipped with a TLD (NSD model)

where,

$$RE = 1-\beta^2-\mu\beta^2\frac{\gamma^2\left(\gamma^2-\beta^2+(2\zeta_d\beta)^2\right)}{\left(\gamma^2-\beta^2\right)^2+(2\gamma\zeta_d\beta)^2},$$
$$IM = 2\zeta_s\beta+\frac{2\mu\gamma\zeta_d\beta^5}{\left(\gamma^2-\beta^2\right)^2+(2\gamma\zeta_d\beta)^2}, \tag{4.4}$$

$$\omega_s=\sqrt{\frac{k_s}{m_s}},\quad \omega_d=\sqrt{\frac{k_d}{m_d}},\quad \zeta_s=\frac{c_s}{2\sqrt{k_s m_s}},\quad \zeta_d=\frac{c_d}{2\sqrt{k_d m_d}},$$
$$\mu=\frac{m_d}{m_s},\quad \beta=\frac{\omega}{\omega_s},\quad \gamma=\frac{\omega_d}{\omega_s}. \tag{4.5}$$

To normalize Equation (4.3), the peak displacement of the structure without TLD is introduced

$$x_{0,wo}=\frac{F_0}{k_s}\frac{1}{\sqrt{(1-\beta^2)^2+(2\zeta\beta)^2}}. \tag{4.6}$$

The resonance peak displacement of the structure without TLD can be calculated by

$$A_0 = \frac{F_0}{k_s} \frac{1}{2\zeta_s \sqrt{1-\zeta_s^2}} \,. \tag{4.7}$$

The normalized peak displacement of the structure is obtained by dividing Equation (4.3) by (4.7) and expressed as

$$x_0' = \frac{x_0}{A_0} = \frac{2\zeta_s \sqrt{1-\zeta_s^2}}{\sqrt{RE^2 + IM^2}} \,. \tag{4.8}$$

Because ζ_d and γ are functions of x_0, an iteration procedure is required to solve Equation (4.8). A simple iteration procedure is illustrated in Figure 4.11. The initial value of x_0 is

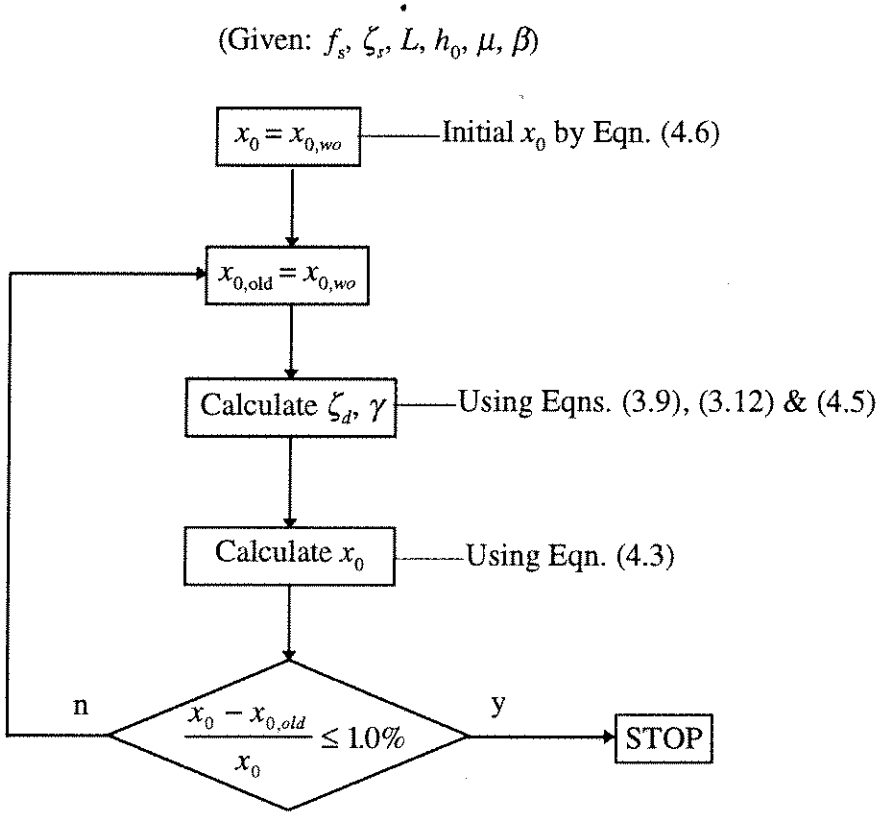

Figure 4.11 A solution procedure for the frequency responses of a structure coupled with a TLD as the structure is subjected to harmonic excitations. The TLD is characterized by the NSD model.

set to the peak displacement of the structure without the TLD calculated using Equation (4.6). Iteration stops as the calculated x_0 converges to the assumed x_0: in this study, the convergence criterion of 1.0 % is applied.

The effectiveness of the TLD is measured in terms of reduction in the maximum peak displacement of the structure due to the TLD as

$$\Psi = 1 - \max(x_0') \ . \tag{4.9}$$

4.2.2 TLD tuning - linear tuning and nonlinear tuning

In practice, the size of the tank is selected based upon construction considerations. The water depth is calculated to tune the TLD to the structure using the linear shallow-water wave theory. This is referred to as "linear tuning" of the TLD because the linear fundamental natural frequency of the TLD is tuned to the fundamental natural frequency of the structure. The linearly tuned water depth for the given size of the tank is calculated from Equation (2.1):

$$h_0 = \frac{L}{\pi} \tanh^{-1}\left(\frac{4\pi}{g} L f_s^2\right) . \tag{4.10}$$

As discussed in the previous chapters, the real (or nonlinear) natural frequency of the TLD shifts from the linear natural frequency as a function of the excitation amplitude (See Equation (3.12)). The "nonlinear tuning" of the TLD is defined as: tuning the nonlinear fundamental natural frequency of the TLD to the fundamental natural frequency of the structure. From Equations (2.1) and (3.3), the nonlinear fundamental natural frequency is expressed as

$$f_d = \frac{\xi}{2\pi} \sqrt{\frac{\pi g}{L} \tanh \frac{\pi h_0}{L}} \ . \tag{4.11}$$

If the TLD is characterized by the NSD model, it is assumed that the nonlinear fundamental natural frequency f_d is related to the structural frequency f_s by the optimum tuning ratio, γ_{opt} for a TMD[1] as follows:

$$f_d = \gamma_{opt} f_s \ . \tag{4.12}$$

Combining Equations (4.11) and (4.12), the nonlinearly tuned water depth for the given size of the tank can be estimated by:

$$h_0 = \frac{L}{\pi} \tanh^{-1}\left(\frac{4\pi}{g} \frac{\gamma_{opt}^{\ 2}}{\xi^2} L f_s^{\ 2} \right) . \tag{4.13}$$

In this equation, h_0 is a function of ξ which is a function of excitation amplitude. Therefore, an iteration procedure is required to determine the nonlinearly tuned water depth h_0.

4.2.3 TLD performance for harmonic excitations

Steady-state responses of a structure equipped with a TLD can be obtained by solving Equation (4.8) using the proposed iteration solution scheme as described in Figure 4.11. For the given structural properties (f_s, ζ_s) and the mass ratio (μ), the structural response is a function of L, h_0 and β. The normalized structural responses also depend on the excitation amplitude because of the nonlinear characteristics of the TLD. In this section, performance of various TLDs attached to a lightly damped SDOF structure are evaluated by comparing sweep frequency responses of the structure for each TLD. The performance is measured in terms of the effectiveness as described in Equation (4.9).

A structure with natural frequency f_s = 0.32 Hz and damping ratio ζ_s = 1.0 % was selected.[2] The mass ratio μ of the TLD to the structural mass is set equal to 1.0 %. Because the property of the TLD depends on the excitation amplitude as shown in

---

[1] See Appendix B.2 for γ_{opt}

[2] The property of the selected structure is adopted from the Shin Yokohama Prince Hotel (Wakahara, 1992)

Equations (3.9) and (3.10), two different excitation amplitudes were employed. The excitation amplitudes were determined such that the maximum peak accelerations of the structure with a linearly tuned liquid damper becomes the designated values, $\ddot{x}_s$ = 20 or 3 milli-g. The corresponding maximum peak displacements for the selected structure can be calculated as $x_{s,0} = \frac{\ddot{x}_s}{\omega^2}$ = 4.85 or 0.73 cm. By estimating 60 % reduction in the peak acceleration due to a linearly tuned liquid damper, the maximum peak displacement of the structure without a TLD is estimated as $A_0 = \frac{x_{s,0}}{(1-0.6)}$ = 12.13 or 1.82 cm. The amplitude of the harmonic forcing, F_0, was determined such that the maximum peak displacement A_0 of the structure without a TLD becomes 12.13 or 1.82 cm, respectively, by using the equation:

$$F_0 = A_0 k_s 2\zeta_s \sqrt{1-\zeta_s^2} \quad . \tag{4.14}$$

Two different sizes of TLDs (L = 171 and 300 mm) were employed for each excitation amplitude. Three different water depths were selected for each tank such that each TLD is linearly tuned, nonlinearly tuned or mis-tuned. The linearly tuned water depth was determined using Equation (4.10). The nonlinearly tuned water depth was determined using Equation (4.13). The mis-tuned water depth was selected to simulate the condition of approximately 10 % miscalculation in the water depth from the nonlinearly tuned value. The characteristics of the selected TLDs and excitation amplitudes are described in Table 4.2.

The results of the analyses for the frequency responses of the structure for each case are plotted in Figure 4.12 and 4.13 for each excitation amplitude, respectively. The plotted quantities are the responses normalized to the maximum response of the structure without the TLD. The resulting properties and effectiveness of each TLD are tabulated in Table 4.2. The results are summarized as follows:

- The performance of the TLD depends on the excitation amplitude. For example, the TLD with L = 171 cm and h_0 = 12.4 cm demonstrates an effectiveness level of 60 % and 70 % at acceleration level $\ddot{x}_s$ = 20 or 3 milli-g, respectively. In these limited cases, TLDs perform better at a lower excitation amplitude because the TLDs develop the damping ratios close to the optimum values at the acceleration level $\ddot{x}_s$ = 3 milli-g.
- The performance of the TLD is maximized by nonlinear tuning. For a given size of a tank, nonlinear tuning is achieved by adjusting the water depth.

Table 4.2 Properties and performance of TLDs attached to a structure at resonance. (f_s = 0.32 Hz, ζ_s = 1.0 %, μ = 1.0 %)

Data						Results			
(*1)	Tank		Linear		Tuning	Nonlinear			Effectiveness
$\ddot{x}_s$ (milli-g)	L (cm)	h (cm)	$f_{d,lin}$ Hz	γ_{lin}	Type	ζ_d (%)	κ	γ	ψ (%)
20	171	12.4	0.32	1.00	(*1)	15	1.04	1.02	60
		11.6			(*2)	15	1.04	0.99	63
		10.5			(*3)	15	1.04	0.94	60
	300	39.7	0.32	1.00	(*1)	12	1.04	1.02	65
		36.8			(*2)	11	1.04	0.99	69
		33.0			(*3)	12	1.04	0.94	63
	600	180			(*2)	8.3	1.04	0.99	75
3	171	12.4	0.32	1.00	(*1)	6.8	1.02	1.02	70
		11.6			(*2)	6.3	1.03	0.98	76
		10.5			(*3)	7.3	1.03	0.94	63
	300	39.7	0.32	1.00	(*1)	5.6	1.03	1.01	70
		36.8			(*2)	5.3	1.03	0.98	74
		33.0			(*3)	6.2	1.04	0.93	60

Notes: *1. Linearly tuned, i.e., γ_{lin} = 1.0
*2. Nonlinearly tuned, i.e., γ = 0.99
*3. Mis-tuned, i.e., γ < 0.99
*4. Estimated structural acceleration in *milli-g*.

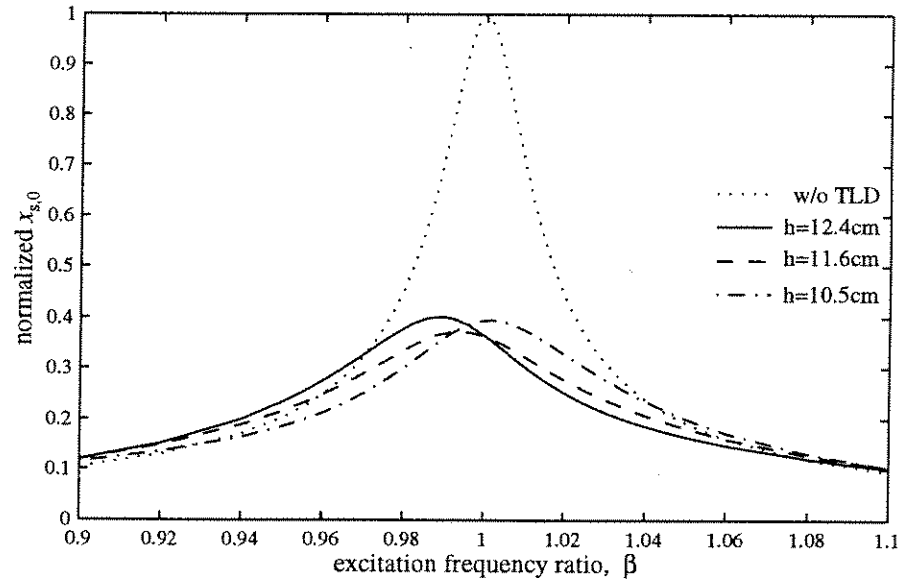

(a) $L = 171$cm

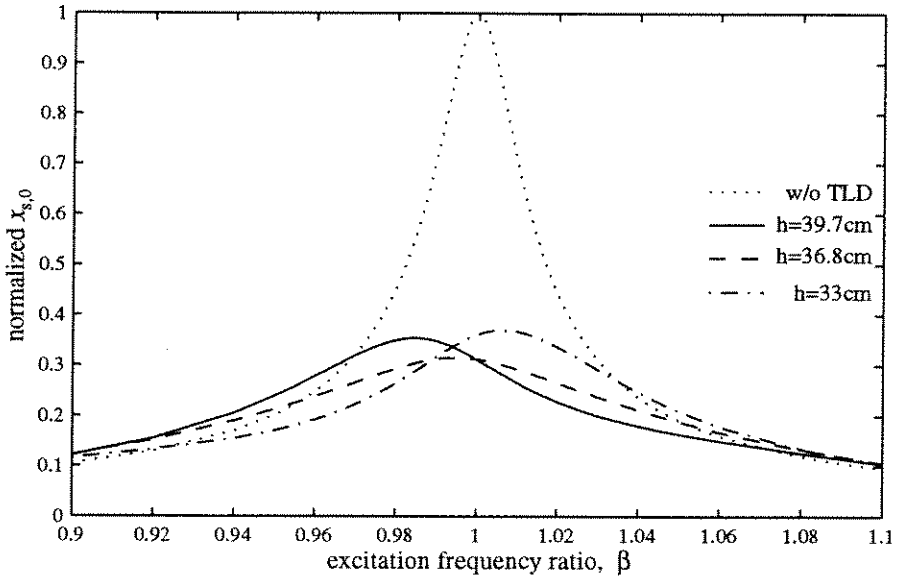

(b) $L = 300$cm

Figure 4.12 Frequency responses of the structure coupled with various TLDs. The natural frequency and the damping ratio of the structure are f_s=0.32 Hz and ζ_s=1.0 %. The mass ratio, μ=1.0%. The estimated maximum acceleration of the structure with the TLD, $x_{0,max}$ is approximately 20 *milli-g*.

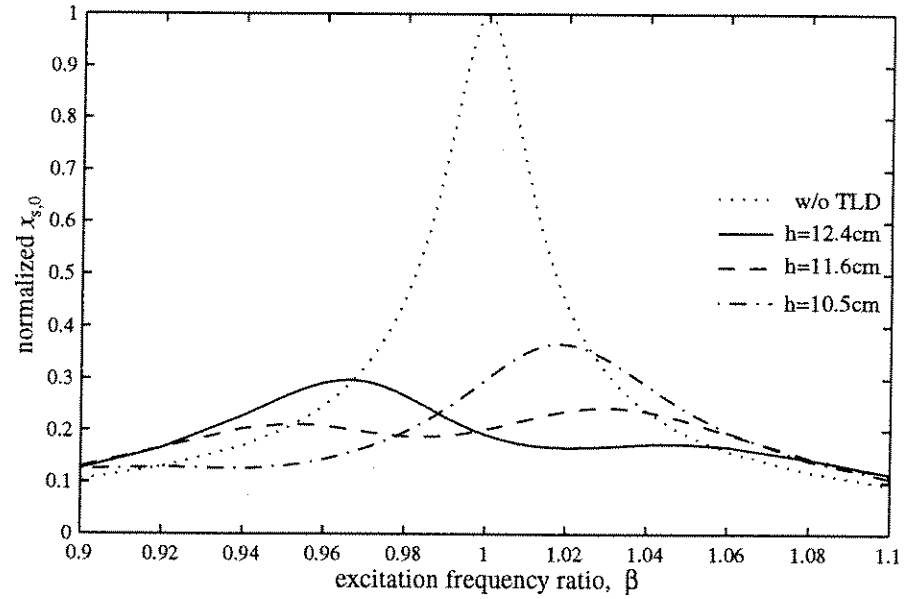

(a) $L = 171$cm

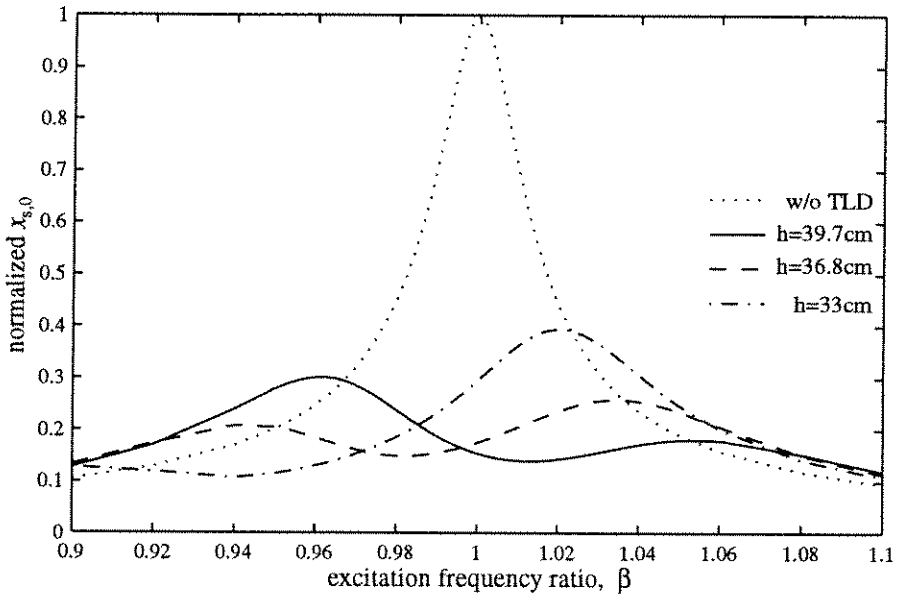

(b) $L = 300$cm

Figure 4.13 Frequency responses of the structure coupled with various TLDs. The natural frequency and the damping ratio of the structure are f_s=0.32 Hz and ζ_s=1.0 %, respectively. The mass ratio μ=1.0%. The estimated maximum acceleration of the structure with the TLD $x_{0,max}$ is approximately 3 *milli-g*

- The performance of TLD depends on the tank size. For example, the nonlinearly tuned TLDs with L = 171 cm and 300 cm demonstrate the effectiveness of 63 % and 69 %, respectively, at the acceleration level $\ddot{x}_s$ = 20 milli-g. In this case, the larger TLD performs better because it develops the damping ratios closer to the optimum values than the smaller one. However, at the acceleration level $\ddot{x}_s$ = 3 milli-g, the performance of both TLDs are at similar levels because their damping values are similar. Both TLDs demonstrate the higher effectiveness level, i.e., Ψ = 76 % and 74 %, respectively, because the damping ratios of both TLDs at this acceleration level are close to the optimum value.
- The TLDs at acceleration level $\ddot{x}_s$ = 20 milli-g develops high damping compared to the optimum value. To lower the damping value of the TLD, the tank size was increased to L = 600 cm. This TLD develops the damping ratio 8.3 % which is close to the optimum value and increases the effectiveness to 75 %.
- The mis-tuned TLDs have lower effectiveness for all cases.

4.2.4. TLD design guide for harmonic excitations

Consider a SDOF structure equipped with a linear mechanical damper. The normalized peak displacement of the structure x_0' as shown in Equation (4.8), is a function of μ, ζ_s, ζ_d, γ, and β. The normalized maximum structural displacement $x_{0,\max}'$ is defined as the maximum value of x_0' over sweep excitation frequencies. With given values of μ and ζ_s, $x_{0,\max}'$ is expressed as a function of ζ_d and γ.

The plots of $x_{0,\max}'$ vs. ζ_d of the linear system with various tuning ratios make a family of design curves as shown in Figure B.2 in Appendix B. In Figure 4.14, the curves for two values of tuning ratios (γ = 0.99 and 1.02) are plotted for the cases used in the previous section, i.e., f_s=0.32 Hz, ζ_s=1.0 % and μ=1.0 %.

The results from the case studies for the linearly and nonlinearly tuned TLDs with various sizes in the previous section are shown in this family of curves. The results described in Table 4.2 for the TLDs at acceleration level $\ddot{x}_{s,\max}$ = 20 milli-g are plotted in Figure 4.14 (a). In particular, the result for the linearly tuned TLD with length L=171 mm, ζ_d = 15 % and γ = 1.02 is identified in Figure 4.14 (a) with the label of L171h12.4. The normalized maximum structural displacement $x_{0,\max}{}'$ is 0.40 which corresponds to an effectiveness of the TLD of ψ = 60 %. This agrees with the value in Table 4.2 which was obtained from the frequency response analyses. Table 4.2 identifies ζ_d = 15 % and γ = 0.99 for the nonlinearly tuned TLD with the same size tank. These values are plotted with a cross-mark with the label of L171h11.6. An effectiveness of 63 % is identified from the figure, which agrees with the value in Table 4.2. The results from several other cases are shown in Figure 4.14(a) in the same manner. The nonlinearly tuned TLD with tank length L = 600 cm develops the values of ζ_d = 8.3 % and γ = 0.99 and the highest effectiveness of ψ = 75 %. Figure 4.14 (b) contains the plots of the results for the TLDs at excitation amplitude $\ddot{x}_{s,\max}$ = 3 milli-g in the same manner as described above. It is observed from this study that:

- There exists a TLD that performs most effectively under a harmonic excitation at a particular amplitude of excitation. The optimum parameters for the linear TMD hold true for the NSD model at steady-state.
- The effectiveness of a TLD at steady-state can be estimated using the design chart alone without further analysis.
- The nonlinear tuning significantly enhances the performance of the TLD as the damping ratio of the NSD model approaches the optimum value for the TMD.

Based upon the results of this numerical study, an iteration procedure was developed to select the most effective TLD for a given excitation amplitude. This design procedure is illustrated in Figure 4.15.

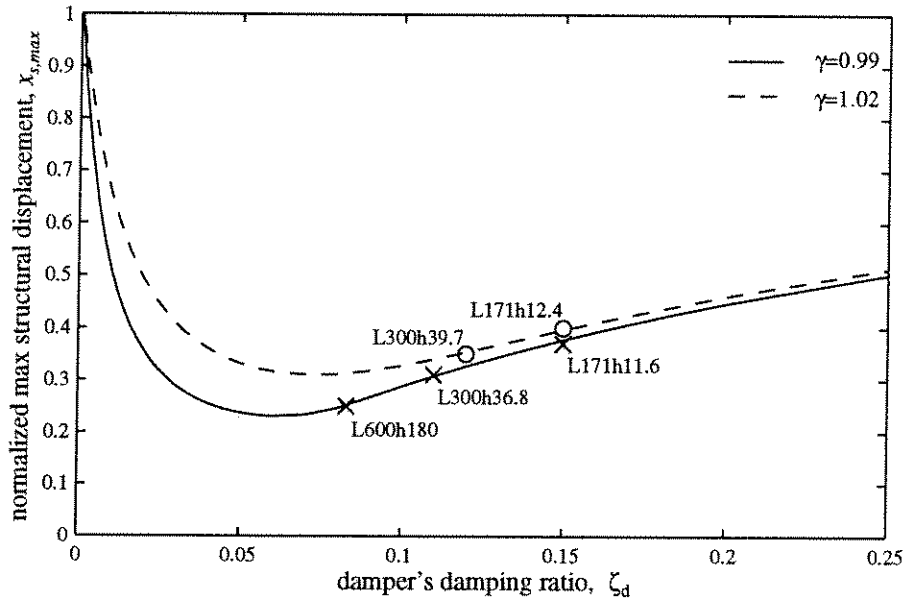

(a) $\ddot{x}_{s,\max}$ = 20 milli-g

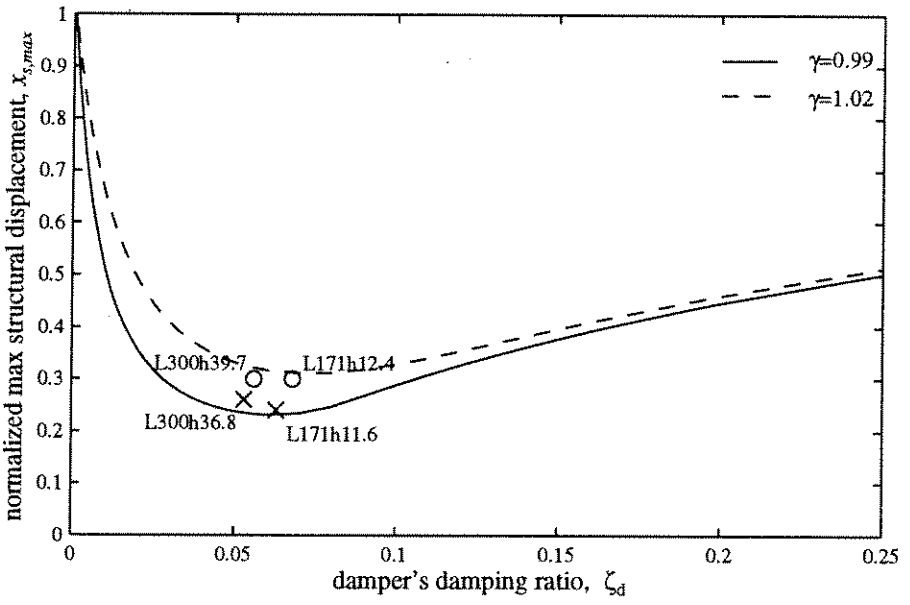

(b) $\ddot{x}_{s,\max}$ = 3 milli-g

Figure 4.14 Maximum structural displacements. Curves are for the structure equipped with linear TMDs with various tuning ratios. Circle-marks are for the structure equipped with linearly tuned liquid dampers. Cross-marks are for the structure equipped with nonlinearly tuned liquid dampers. The damping ratio of the structure, ζ_s=1.0 %. The mass ratio, μ=1.0 %.

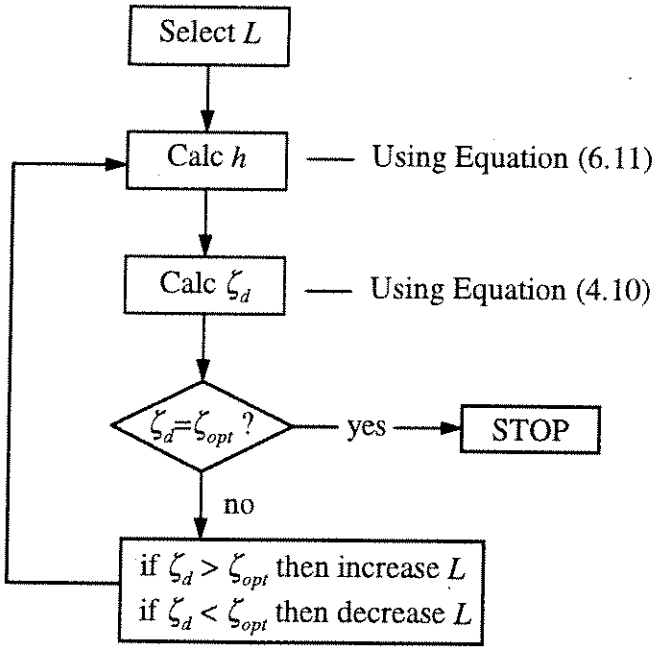

Figure 4.15 A scheme for selection of the most effective TLD for a given excitation amplitude. The TLD is characterized by an NSD model.

4.3 TLD performance and design procedure for white noise excitations

In this section, the behavior of the TLD coupled with a lightly damped SDOF structure is investigated for white noise excitation. An approximation solution scheme coupled with spectral analysis for the combined system is developed. The effectiveness is measured in terms of the reduction of the RMS value of the structural displacement. The approximation scheme is calibrated using the results from time-history analyses of the TLD.

4.3.1 Time history analysis

Consider a SDOF structure equipped with a TLD. The system can be modeled as a two-degree-of-freedom system using the NSD model for the TLD as shown in Figure 4.10. As the structure is subjected to a random forcing with a constant spectral density (white noise forcing), the equation of motion is written as Equation (4.2) and can be numerically solved as described in Section 4.1.

Fifty sets of 1200 Normally distributed random numbers with zero mean and unit variance were generated[1]. Each set of random numbers were smoothed using a cubic-spline fitting scheme. Twenty four equally distributed data points between each random number were added. Setting the time step between each data point equal to Δt=0.02 second, each data set becomes a 600-second white noise random number series.

The generated 50 sets of random number series were imposed as forcing functions on a SDOF structure equipped with various TLDs. The structure and TLDs which were employed for the case studies under harmonic excitation in Section 4.2.3 were selected, i.e., f_s=0.32 Hz, ζ_s=1.0 %, μ = 1.0 %, linearly or nonlinearly tuned TLDs with L=171 cm or 300 cm. The magnitudes of the random forcing functions were adjusted by trial and error such that the estimated maximum peak acceleration of the structure equipped with a

[1] Refer to the Matlab command "randn".

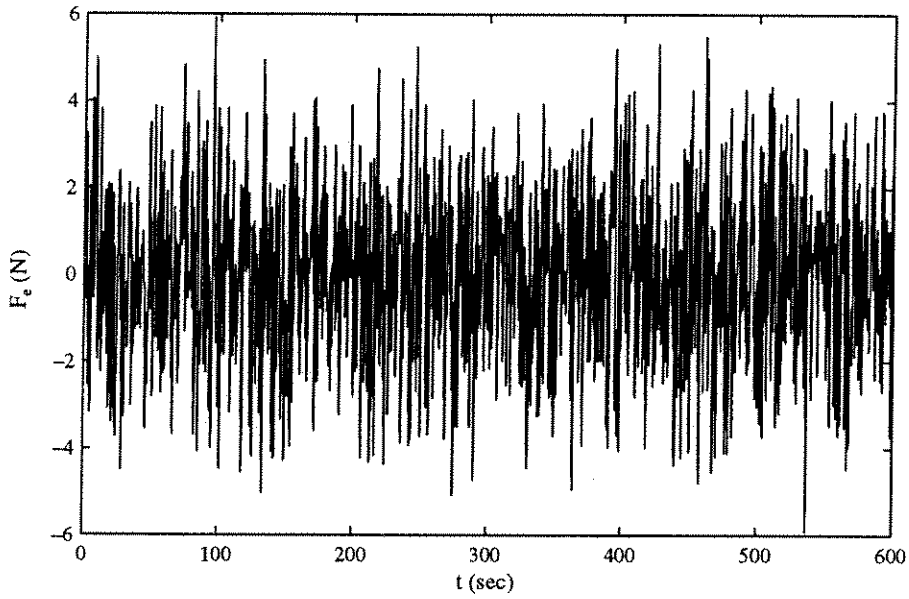

(a) White noise random forcing

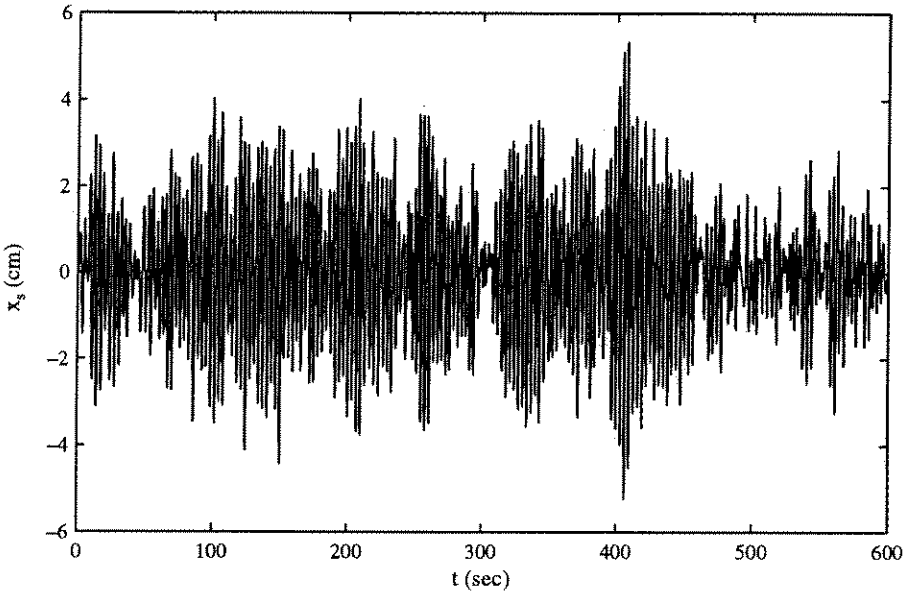

(b) Structural displacement induced by the random forcing

Figure 4.16 Sample plots of a generated white noise random forcing and the structural motion induced by the random forcing.

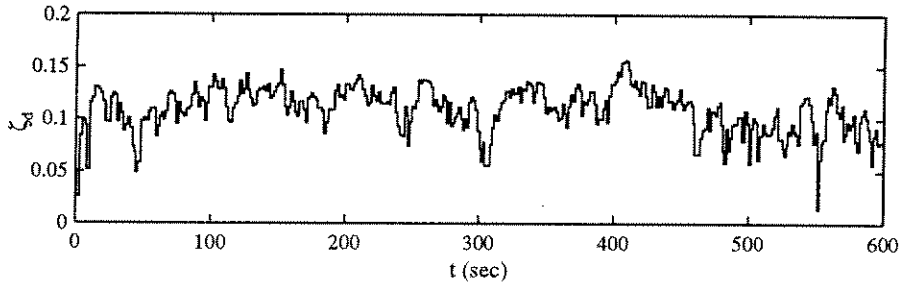

(a) Damping ratio, ζ_d

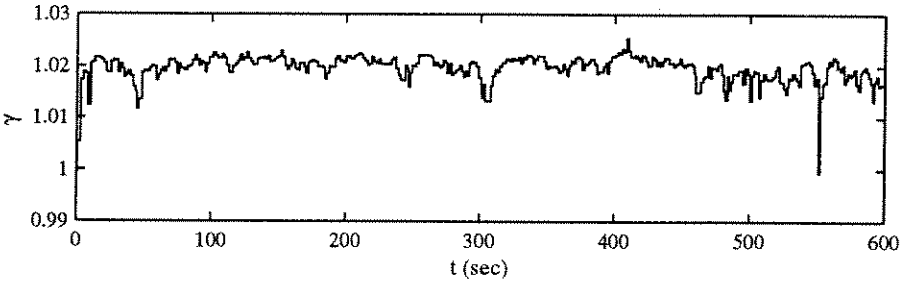

(b) Tuning ratio, γ

Figure 4.17 Sample time histories for the damping ratio and tuning ratio of the NSD model for the system described in Figure 4.16.

linearly tuned TLD with length L = 171 cm becomes 20 milli-g. One sample set of the generated random forcing function is plotted in Figure 4.16(a).

The adjusted random forcing functions were applied to the selected structural system equipped with TLDs. A sample time history of the structural displacements was plotted in Figure 4.16(b). The corresponding plots for the damping ratio ζ_d and frequency ratio γ of the NSD model are shown in Figure 4.17. After 300 seconds, the time histories for the structural responses and the stiffness and damping coefficients of the NSD model were recorded. The average results of the 50 loading cases were tabulated in Table 4.3.

Table 4.3 Responses of a SDOF structure with various TLDs under white noise excitation obtained from time history analyses.
(f_s = 0.32 Hz, ζ_s = 1.0 %, μ = 1.0 %, targeted $\ddot{x}_{s,\max}$ =20 milli-g)

		L=171 cm		*L*=300 cm	
		h=12.4 cm (*1)	*h*=11.6 cm (*2)	*h*=39.7 cm (*1)	*h*=36.8 cm (*2)
x_s	rms (cm)	1.42	1.39	1.37	1.34
	max peak(cm)	4.56	4.44	4.44	4.30
	average peak (cm)	1.76	1.72	1.70	1.66
	max peak factor (α_{max})	3.21	3.20	3.24	3.22
	avg peak factor (α_{avg})	1.24	1.24	1.24	1.24
	reduction in rms (%)	34	36	36	38
	reduction in max (%)	27	29	29	31
$\ddot{x}_s$	rms (cm/s^2)	5.84	5.75	5.64	5.56
	max peak(cm/s^2)	19.3	18.8	18.7	18.3
	average peak (cm/s^2)	8.01	4.3.91	4.3.78	4.3.69
	max peak factor (α_{max})	3.30	3.27	3.32	3.29
	avg peak factor (α_{avg})	1.38	1.38	1.38	1.39
	reduction in rms (%)	34	35	36	37
	reduction in max (%)	27	28	29	30
ζ_d	average (%)	10.2	10.1	8.3	8.2
γ	average	1.02	0.99	1.02	0.98

Notes: (*1). Linearly tuned

(*2). Nonlinearly tuned

The maximum and average peak factors were defined as the ratio of the maximum and average peak responses, respectively, to the RMS (root mean square) response. The effectiveness is defined as the percent reduction of the RMS value of the structural displacement compared to the structure without TLD. In addition, the reductions of maximum displacement, RMS and maximum acceleration of the structure are presented for reference. The average values of ζ_d and γ of the NSD model during the recorded time duration for each TLD case were calculated and presented. The following summarize observations from the limited case studies:

- The maximum and average peak factors in the structural displacement were estimated as 3.2 and 1.25, respectively. These values will be used in the spectral analysis in the next section.
- The nonlinear tuning method developed for harmonic excitation as described in Equation (4.13) is also valid for white noise excitation, i.e., the tuning ratio of the NSD model of a nonlinearly tuned TLD approaches the optimal value for the linear TMD system.
- The damping of the NSD model can be adjusted by tank length.
- The effectiveness of the TLD increases as the ζ_d and γ of the NSD model approach the optimum values for the linear TMD system.

A detailed discussion about the effectiveness of the TLD will be presented in the next section.

4.3.2 Spectral analysis

The mean square response of a stationary process for a linear system under white noise excitation is calculated by

$$E[x_s^2] = S_0 \int_{-\infty}^{\infty} \left| H_{x_s}(\omega) \right|^2 d\omega \ , \tag{4.15}$$

in which S_0 is the constant spectral density of the random input forcing and $H_{x_s}(\omega)$ is the frequency response function of the structure. As described in Appendix C, the root mean square (RMS) response (displacement, $E\left[\sqrt{x_{s,0}^2}\right]$ *or* $x_{s,rms,wo}$) of the structure without a TLD is expressed as

$$E\left[\sqrt{x_{S,0}{}^2}\right] = \sqrt{\frac{\pi S_0}{2\zeta_s m_s{}^2 \omega_s{}^3}} = \sqrt{\frac{\pi S_0 \omega_s}{2\zeta_s k_s{}^2}} \quad . \tag{4.16}$$

The RMS response of the structure equipped with a TLD is normalized to the RMS response of the structure without TLD. Through the solution procedure described in Appendix C, the normalized RMS displacement ($E'\left[\sqrt{x_s^2}\right]$ *or* $x_{s,rms}$) of the structure is calculated using the formula

$$E'\left[\sqrt{x_s{}^2}\right] = \sqrt{2\zeta_s \overline{\Pi}} \quad , \tag{4.17}$$

where

$$\overline{\Pi} = \frac{-\overline{A}_1 - \overline{A}_3(\overline{B}_1{}^2 - 2\overline{A}_0) + \overline{A}_0(\overline{A}_1 - \overline{A}_2\overline{A}_3)}{\overline{A}_0\overline{A}_3{}^2 + \overline{A}_1{}^2 - \overline{A}_1\overline{A}_2\overline{A}_3} \quad , \tag{4.18}$$

$$\begin{gathered} \overline{A}_0 = \gamma^2; \quad \overline{A}_1 = 2(\zeta_s\gamma^2 + \zeta_d\gamma); \quad \overline{A}_2 = 4\zeta_s\zeta_d\gamma + 1 + \gamma^2(1+\mu); \\ \overline{A}_3 = 2(\zeta_s + \zeta_d(1+\mu)\gamma); \quad \overline{B}_0 = \gamma^2 = \overline{A}_0; \quad \overline{B}_1 = 2\zeta_d\gamma. \end{gathered} \tag{4.19}$$

The normalized RMS displacement of the structure, as described in Equation (4.16), is a function of μ, ζ_s, ζ_d and γ. The values of ζ_d and γ of the NSD model are functions of the peak structural displacement as seen in Equations (3.9) and (3.12). Because of the non-deterministic nature of the structural displacement under random vibration, it is essential to estimate the expected value of the peak structural displacement over a specific time period.

The maximum peak factor α_{max} is defined as the ratio of the maximum peak displacement to the RMS displacement of the structure. The average peak factor α_{avg} is defined as the ratio of the average peak displacement to the RMS displacement of the

structure. The maximum and average peak factors of the structural motion under white noise excitation are estimated from a series of time history analyses. The expected maximum and average peak displacements of the structure can be estimated by multiplying the expected RMS structural displacement by the maximum and average peak factors, respectively. The corresponding values of ζ_d and γ of the NSD model are determined using Equations (3.9) and (3.12).

Figure 4.18 illustrates the schematic diagram of the solution procedure for the given system. Because of the nonlinearity of the TLD, an iterative process is required.

4.3.3 TLD performance under white noise excitation

Sample studies are conducted to evaluate the performance of TLDs interacting with a lightly damped SDOF structure. Equation (4.17) is solved using the proposed stochastic scheme. The convergence criterion for the iteration procedure is set equal to 1.0 %. The effectiveness of the TLD is assessed in terms of the reduction of the RMS displacement of the structure.

From 50 sets of sample time history analyses, which were described in Section 4.3.1, the maximum and average peak factors for the structural displacement were measured as approximately 3.2 and 1.25, respectively. These estimated peak factors are used in these sample studies.

The structure and TLDs which were employed for the case studies of time history analysis in the previous section are used in this investigation, i.e., f_s = 0.32 Hz, ζ_s = 1.0 %, μ = 1.0 % and linearly or nonlinearly tuned TLDs with L = 171 cm or 300 cm. In addition, the same size TLDs but with 10 % under-estimated water depth are investigated. The spectral density of the excitation force is determined such that the estimated maximum peak acceleration of the structure, equipped with a linearly tuned TLD, becomes approximately 20 milli-g. It is accomplished by the following procedure:

If it is assumed that the TLD reduces the maximum peak acceleration by approximately 35 %, the maximum peak acceleration of the structure without a TLD is estimated by

$$\ddot{x}_{s,peak,wo} = \frac{\ddot{x}_{s,peak}}{(1-0.35)} = 30.8\ milli - g\ . \tag{4.20a}$$

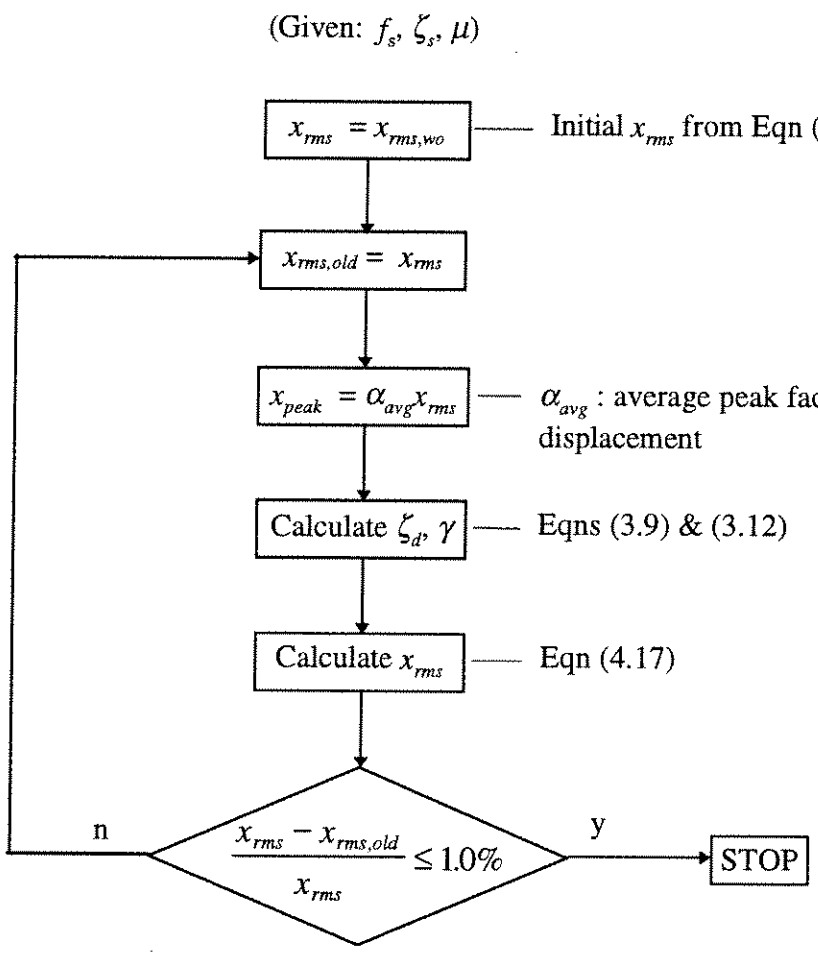

Figure 4.18 A solution procedure for the stochastic responses of a structure coupled with a TLD as the structure is subjected to white noise excitation. The TLD is characterized by the NSD model.

Dividing this result by the estimated maximum peak factor α_{max} = 3.2, the targeted RMS acceleration of the structure without a TLD is estimated by

$$\ddot{x}_{s,rms,wo} = \frac{\ddot{x}_{s,peak,wo}}{\alpha_{\max}} = 9.6\ milli - g\,. \tag{4.20b}$$

The RMS displacement of the structure without a TLD is approximated by

$$x_{s,rms,wo} = \frac{\ddot{x}_{s,rms,wo}}{\omega_s^2} = \frac{(9.62)(0.981)}{(2\,\pi\,0.32)^2} = 2.33\ cm\,. \tag{4.20c}$$

Substituting this result into Equation (4.16), the spectral density of the white noise random forcing is determined as

$$S_0 = \frac{2\zeta_s \cdot \omega_s^3 m_s^2 x_{s,rms,wo}^s}{\pi} = 0.281 \cdot 10^{-4} \cdot m_s^2 \ \left[N^2/\mathrm{sec}\right]. \tag{4.20d}$$

The results of the spectral analyses are tabulated in Table 4.4. In comparing the results with the time history analysis results, it is observed that the spectral analyses yield

Table 4.4 Responses of a SDOF structure with various TLDs under white noise excitation obtained from the proposed stochastic analysis.
(f_s = 0.32 Hz, ζ_s = 1.0 %, μ = 1.0 %, targeted $\ddot{x}_{s,\max}$ =20 milli-g)

		L=171 cm			L=300 cm		
		h=12.4 (*1)	h=11.6 (*2)	h=10.5 (*3)	h=39.7 (*1)	h=36.8 (*2)	h=33.0 (*3)
x_s	rms (cm)	1.43	1.40	1.46	1.38	1.35	1.45
	average peak (cm)	1.78	1.75	1.82	1.72	1.69	1.81
	reduction in rms (%)	39	40	37	41	42	38
ζ_d	average (%)	10.7	10.6	10.8	8.7	8.6	8.8
γ	average	1.02	0.99	0.94	1.02	0.98	0.94

Notes: (*1). Linearly tuned

(*2). Nonlinearly tuned

(*3). Mis-tuned (approximately 10 % error in water depth)

approximately 5 % higher values of the effectiveness of the TLDs. It is assumed that this error is caused by approximations in estimating parameters for the spectral solution procedure.

4.3.4 TLD design procedure for white noise excitation

Consider a SDOF structure equipped with a linear TMD system. The normalized RMS displacement $x_{s,rms}'$ of the structure, as described in Equation (4.17), is a function of ζ_d and γ for the given values of μ and ζ_s. Figure 4.19 contains the plots of $x_{s,rms}'$ vs. ζ_d of the linear TMD system with two values of tuning ratios (γ = 0.99 and 1.02)[1]. The solid curve is for the case with the damper tuning ratio γ of 0.99 which corresponds to the cases with nonlinearly tuned TLDs in Table 4.4. The dashed curve is for the case with the damper tuning ratio γ of 1.02 which corresponds to the cases with linearly tuned TLDs.

The results of the sample case studies using the spectral analyses are shown in Figure 4.19(a). The results from the time history analyses are presented in Figure 4.19(b). As discussed previously, the approximate 5 % over-estimation of the TLD effectiveness from the spectral analysis compared with the time history analysis results is apparent. It is concluded that the most effective TLD for the system under white noise excitation can be determined using the spectral analysis procedure coupled with the searching scheme described in Figure 4.15.

[1] See Figure C.2 for the same plots for the system with various tuning ratios.

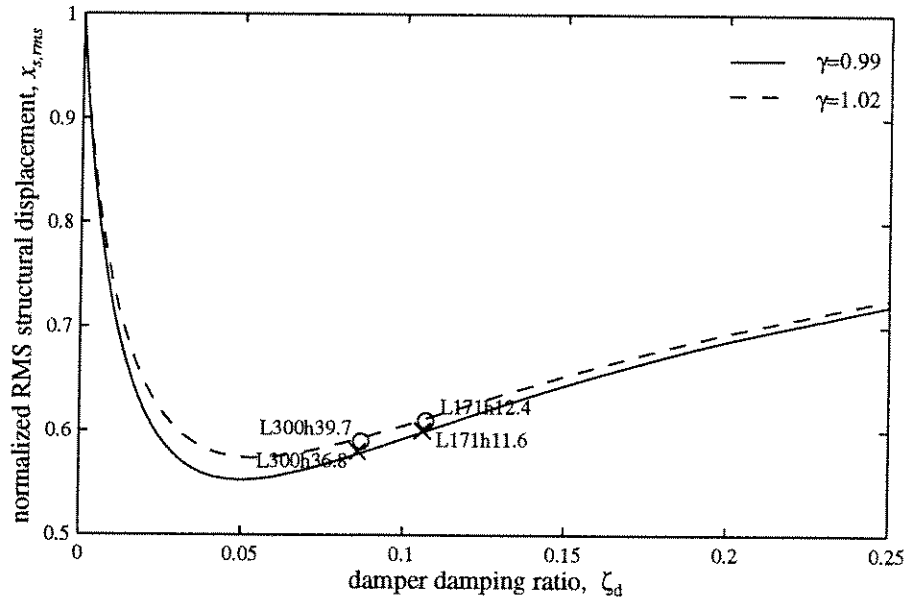

(a) The results from spectral analyses

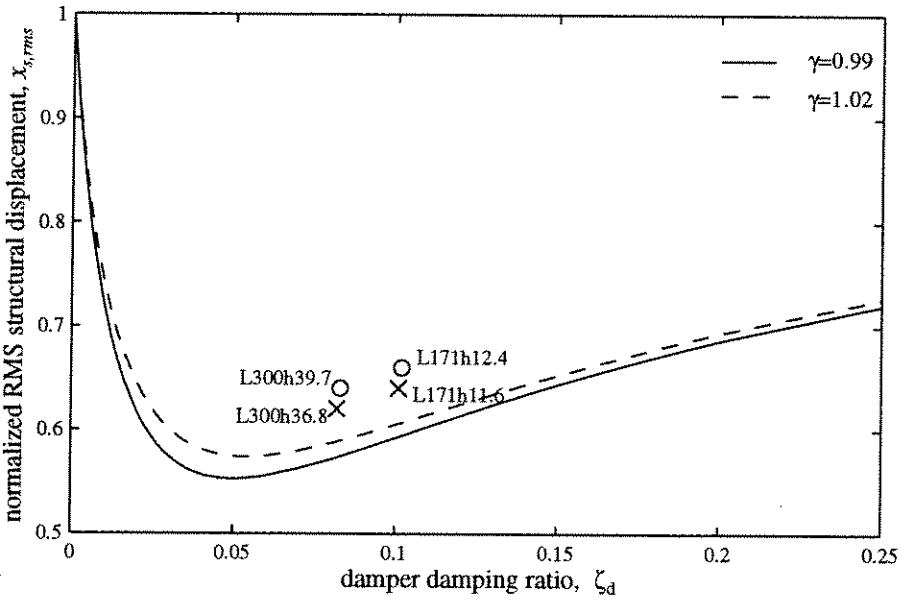

(b) The results from time history analyses

Figure 4.19 The results from sample spectral analyses and time history analyses as compared with a family of curves for the system with a linear TMD system.

4.4 TLD performance under wind conditions

In this section, the performance of TLDs coupled with a lightly damped SDOF structure is investigated using the time series analyses as the structure is subjected to wind pressure loadings. The influence of TLD nonlinearity on its effectiveness is evaluated.

Reed (1983) proposed the ARIMA time series model for wind pressure loadings. For the windward region, Reed proposed an autoregressive model of order 2 (AR(2)) as

$$P_i = \phi_1 P_{i-1} + \phi_2 P_{i-2} + a_t, \tag{4.21}$$

where ϕ_1=1.1450, ϕ_2=-0.2369 and a_t indicates a series of Normally distributed random shocks. Using the AR(2) model, 50 sets of time series of wind pressure loadings were generated. Each series is composed of 30,000 numbers. Setting the sample interval equal to $\Delta t = 0.02$ second, each data set covers 600-seconds.

To investigate the performance of the TLD under wind conditions, the generated wind pressure series were imposed on a SDOF structure equipped with a TLD. By modeling the TLD as the NSD model, the equation of motion of the system is written as Equation (4.2). The dynamic response of the structure were obtained by numerically solving the equation as described in Section 4.1.1.

A SDOF structure and TLDs which were employed for the case studies under harmonic or white noise excitations in the previous sections were selected, i.e., f_s = 0.32 Hz, ζ_s = 1.0 %, μ = 1.0 % and linearly and nonlinearly tuned TLDs with length L = 171 cm and 300 cm, respectively. The data for the case studies are tabulated in Table 4.5.

Because of the nonlinear characteristics of the TLD, the target excitation amplitude was determined first. In this case study, the behavior of the TLD for the maximum structural acceleration of 20 milli-g was targeted. The magnitudes of the wind pressure series were adjusted by trial and error such that the estimated maximum peak acceleration of the structure equipped with a linearly tuned TLD became approximately targeted 20 milli-g.

A sample set of the simulated time series for wind pressure is presented in Figure 4.20(a). The corresponding displacements of the structure equipped with a TLD are presented in Figure 4.20(b). The corresponding plots for the damping ratio ζ_d and tuning ratio γ of the NSD model are shown in Figure 4.21.

Table 4.5 Responses of a SDOF structure with various TLDs as the structure is subjected to wind. (f_s = 0.32 Hz, ζ_s = 1.0 %, μ = 1.0 %, targeted $\ddot{x}_{s,\max}$ =20 milli-g)

		L=171 cm		*L*=300 cm	
		h=12.4 cm (*1)	*h*=11.6 cm (*2)	*h*=39.7 cm (*1)	*h*=36.8 cm (*2)
x_s	rms (cm)	2.12	2.08	2.07	2.02
	max (cm)	7.01	6.89	6.86	6.72
	average peak (cm)	2.17	2.11	2.10	2.03
	peak factor	3.30	3.31	3.31	3.31
	reduction in rms (%)	26	27	28	29
	reduction in max (%)	21	22	22	24
$\ddot{x}_s$	rms (cm/s^2)	6.81	6.65	6.54	6.40
	max (cm/s^2)	21.8	21.3	21.2	20.6
	average peak (cm/s^2)	9.20	9.04	8.91	8.76
	peak factor	3.21	3.2	3.24	3.22
	reduction in rms (%)	34	37	38	40
	reduction in max (%)	27	30	29	33
ζ_d	average (%)	10.7	10.6	8.7	8.6
γ	average	1.02	0.99	1.02	0.98

Notes: (*1). Linearly tuned

(*2). Nonlinearly tuned

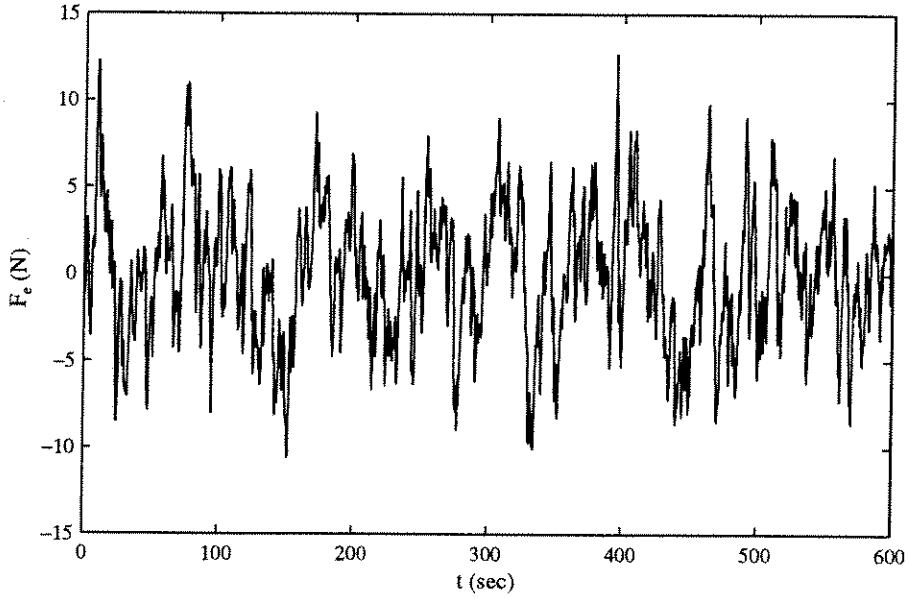

(a) Simulated time series for wind pressure

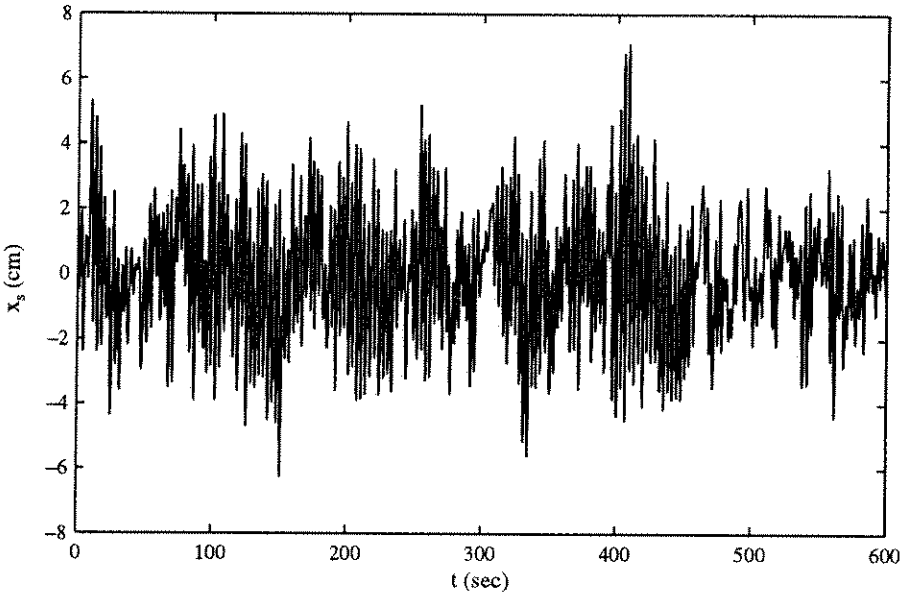

(b) A time series of the displacement of the structure with a TLD

Figure 4.20 A sample set of the simulated time series for wind pressure using the AR(2) model and the structural displacement with a TLD under this wind pressure loading. The properties of the structure and the TLD are: f_s = 0.32 Hz; ζ_s = 1.0 %; μ = 1.0 %; L = 171 cm; h = 12.4 cm.

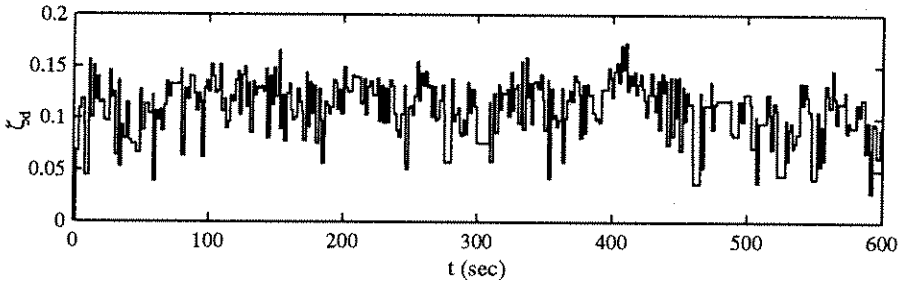

(a) Damping ratio, ζ_d

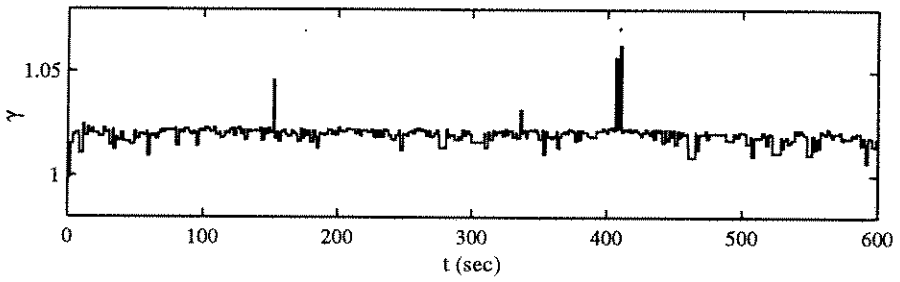

(b) Tuning ratio, γ

Figure 4.21 Time histories of ζ_d and γ of the NSD model for the case of Figure 4.20.

It is assumed that the TLD activated fully after 300 seconds. The time histories of the structural responses and the stiffness and damping coefficients of the NSD model were recorded. The average results of the 50 loading cases for each system are tabulated in Table 4.5. The peak factors were defined as in the previous section. To assess the effectiveness of the TLD, the reduction in the RMS and the maximum values of the displacement and acceleration of the structure equipped with each TLD were compared to those of the same structure without the TLD. The average damping ratio ζ_d and tuning ratio γ of the NSD model for each case were estimated.

The results described in Table 4.5 display trends similar to those observed in the time history analyses of the TLD for white noise excitation. To summarize:

- The nonlinear tuning method developed for harmonic excitation as described in Equation (4.13) is also valid for AR(2) wind pressure excitation, i.e., the tuning ratio of the NSD model of a nonlinearly tuned TLD approaches the optimal value for the linear TMD system.
- The damping of the NSD model can be adjusted by tank length.
- The effectiveness of the TLD increases as the average values of ζ_d and γ of the NSD model approach the optimum values for the linear TMD system.

4.5 Behavior of the TLD under earthquake excitation

The performance of TLDs attached to a lightly damped structure subjected to earthquake ground motion is investigated. Because the NSD model was derived for the harmonic excitation, validity of the model to an earthquake situation was verified using shaking table experiments prior to the performance investigation.

4.5.1 Validity of the NSD model for the earthquake condition

The NSD model was derived under the conditions of harmonic excitation with sweep frequencies. To verify the effectiveness of the model under earthquake motion, shaking table experiments were conducted.

Consider a SDOF structure equipped with a TLD. As the structure is subjected to earthquake motion, the TLD reacts to the structural motion. To simulate the behavior of the TLD for earthquake motion, the TLD must be excited by the structural motions corresponding to the earthquake. As a SDOF structure is subjected to base excitation, the equation of motion of the system is written as Equation (A.1) in Appendix A. The dynamic responses of the structure can be obtained by numerically solving the equation.

Figures 4.22 (a) and (b) show the ground motions for the 1940 El Centro earthquake obtained from "NCEER Strong-Motion Data Base". These ground motions were imposed numerically on an undamped SDOF structure whose natural frequency is f_s = 0.5 Hz. The dynamic responses of the structure were numerically simulated. Because the maximum allowed displacement of the shaking table is approximately 50 mm, the total structural displacement, x_s, was scaled down such that the maximum absolute value of x_s becomes approximately 40 mm. The scaled shaking table motions were plotted in Figure 4.22 (c).

A TLD with length L = 590 mm and water depth h = 36 mm was mounted on the shaking table as illustrated in Figure 2.1. Its linear fundamental natural frequency is 0.506 Hz which is approximately the same as that of the selected structure. The table was excited in the motions shown in Figure 4.22 (c) which were the scaled total displacements

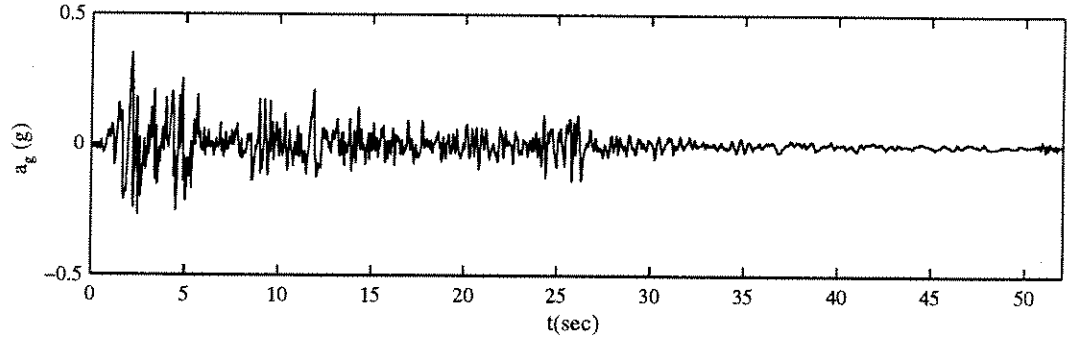

(a) Ground acceleration

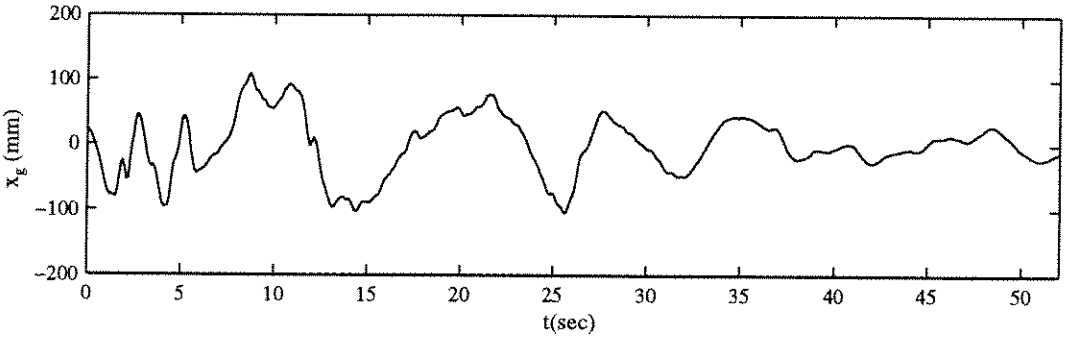

(b) Ground displacement

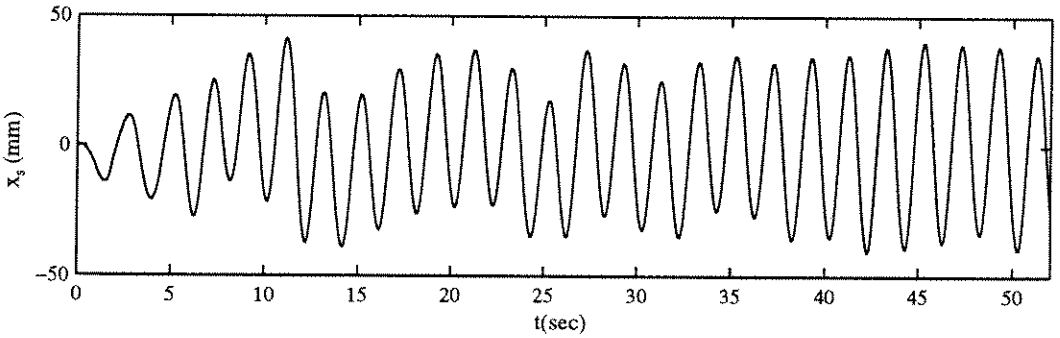

(c) Scaled total structural displacement

Figure 4.22 Ground motions during the El Centro earthquake obtained from "NCEER Strong-Motion Data Base" and scaled total displacements of a undamped structure with natural frequency $f_s = 0.5$ Hz.

of the selected structure under the El Centro earthquake. The base shear generated by the TLD during the entire excitation period was measured with the loadcell and recorded in Figure 4.23 (a) with a solid curve. The amount of energy dissipation due to the base shear during each half cycle was calculated and recorded in Figure 4.23 (b) with a solid curve.

The NSD model for the employed TLD was assumed to be subjected to the same excitation of the shaking table. The equation of motion for the system is expressed as Equation (A.1) in Appendix A. The dynamic responses of the NSD model to the base excitation were obtained numerically. The time history of the base shear generated by the NSD model is presented in Figure 4.23 (a) with a dashed curve. The amount of energy dissipation due to the base shear during each half cycle was calculated and recorded in Figure 4.23 (b) with a dashed curve.

In both plots, it is apparent that the solid curve and the dashed curve are in close agreement. The result indicates that the NSD model which has been derived from the shaking table experiments for harmonic excitations predicts accurately the behavior of the TLD under the El Centro earthquake motion. Figure 4.24 presents the time histories of the damping ratio and the stiffness hardening ratio of the NSD model during the excitation period.

4.5.2 Performance of the TLD under earthquake

Numerical simulation was used to investigate the performance of the TLD attached to a lightly damped SDOF structure subjected to the 1994 Northridge earthquake. The ground motions of the Northridge earthquake obtained from "NCEER Strong-Motion Data Base" and shown in Figure 4.25 are obviously different from the El Centro records. The structure with f_s = 0.32 Hz and ζ_s = 1.0 % was selected. The TLD with length L = 171 cm and water depth h_0 = 11.6 cm was attached to the structure. The mass ratio of the TLD was set equal to μ = 1.0 %.

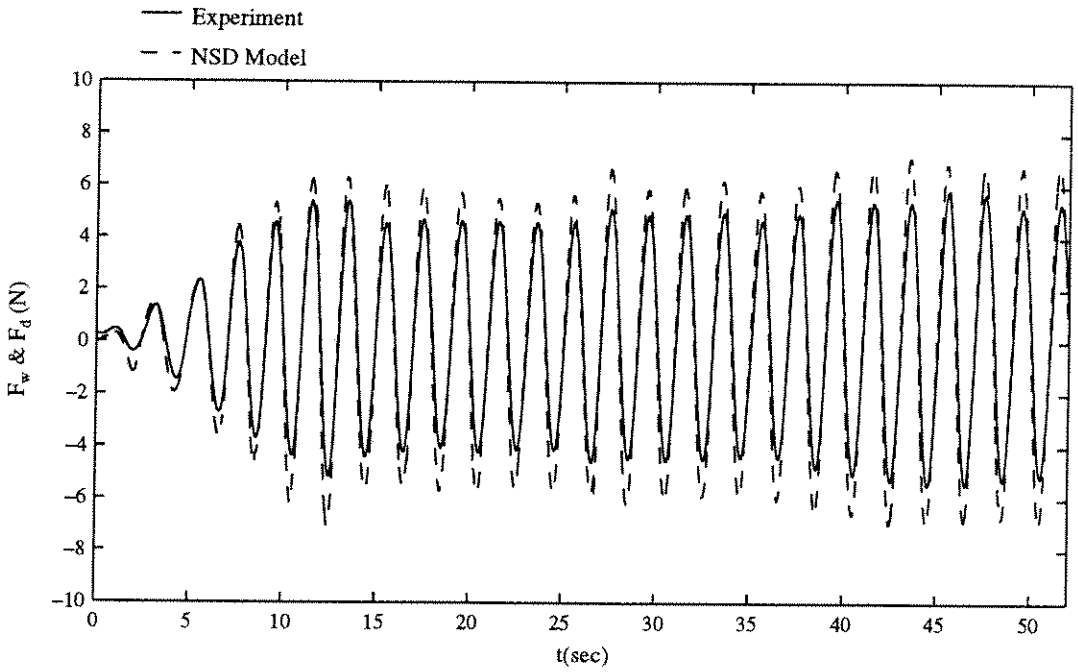

(a) Damping forces

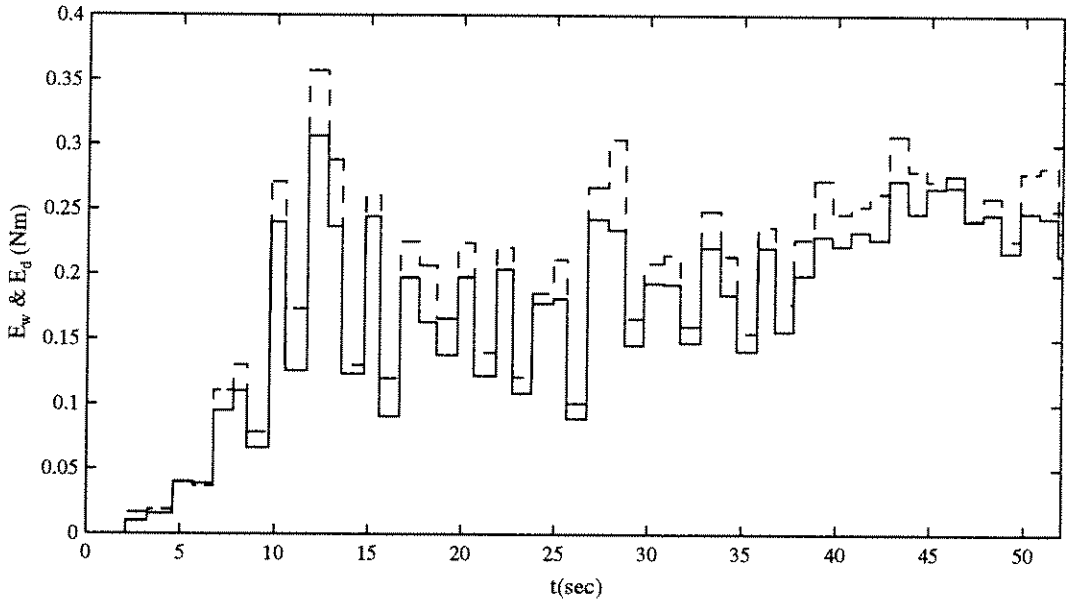

(b) Energy dissipation per cycle

Figure 4.23 Damping forces and energy dissipation per cycle generated by the TLD with the length L = 590 mm, water depth h_0 = 36 mm and its corresponding NSD model. The maximum shaking table displacement $x_{s,max}$ was adjusted to approximately 40 mm.

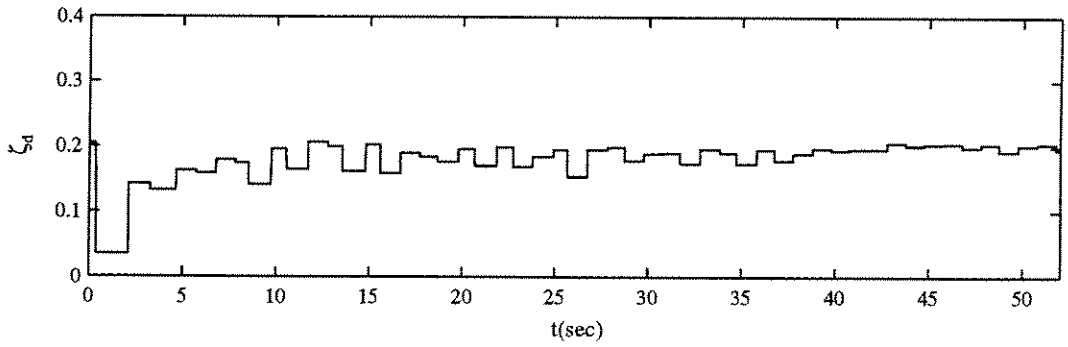

(a) Damping ratio, ζ_d

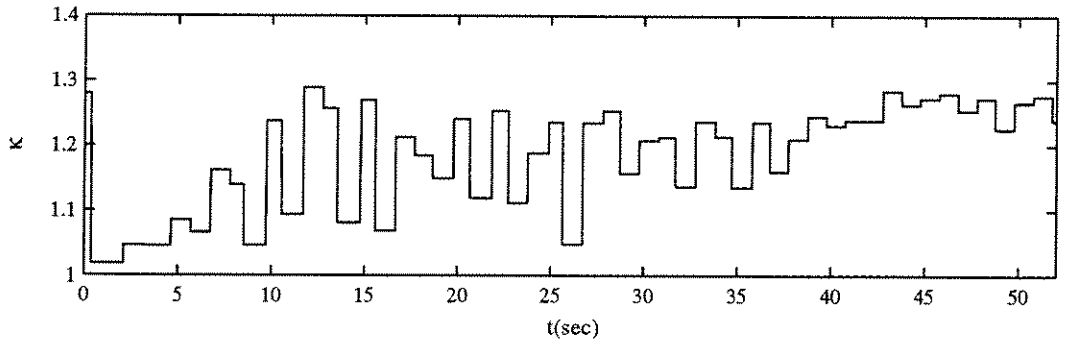

(b) Stiffness hardening ratio, κ

Figure 4.24 Time histories for ζ_d and κ of the NSD model for the case of Figure 4.23.

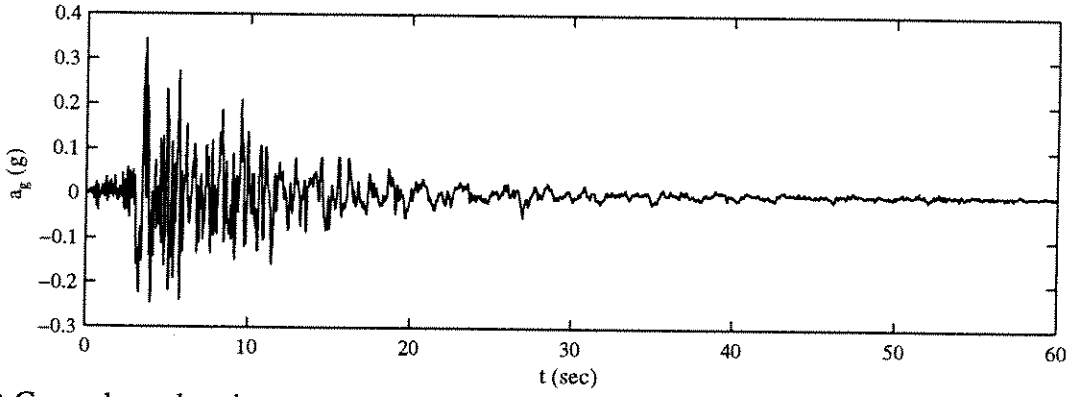

(a) Ground acceleration

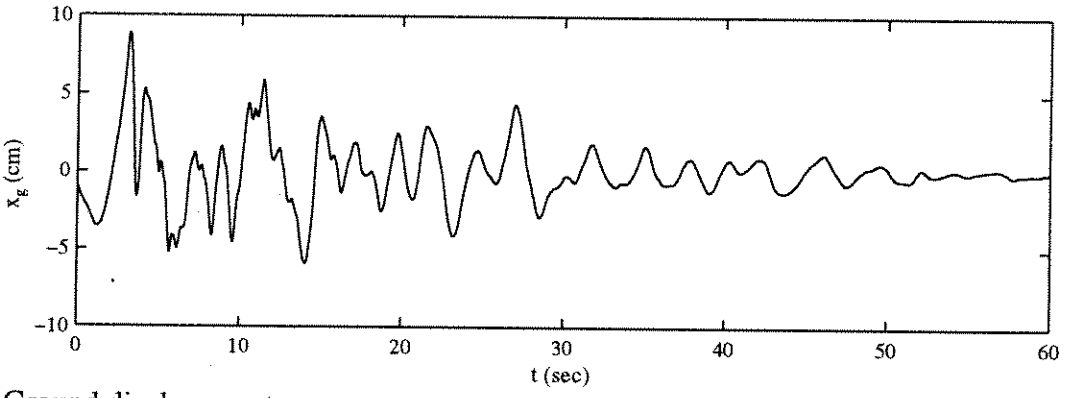

(b) Ground displacement

Figure 4.25 Time history records of ground motions during the 1994 Northridge earthquake. The records were obtained from "NCEER Strong-Motion Data Base - 1990".

By modeling the TLD as a NSD model, the equation of motion of the system is written as in Equation (4.2). The dynamic responses of the structure are obtained by numerically solving the equation as described in Section 4.1. One 60 second record of the responses (displacement and acceleration) of the structure with and without a TLD are plotted together in Figure 4.26. The reduction of the maximum and the RMS responses during every 20 second intervals are averaged and recorded in the plots.

It appears that the TLD does not play any significant role during the initial period of ground motion. This is because the structural motion during this stage is not periodic; consequently, the TLD is not properly tuned to the structural motion. But as time passes, the structural motion becomes more periodic in nature. The TLD which is tuned to the structural natural frequency begins to gain effectiveness. During the last 20 second period, the effectiveness of the TLD increases to approximately 50 % in terms of the RMS displacement or acceleration. However, because the "impact" of the earthquake in the initial seconds is crucial to the structural safety, the TLD must be further investigated to improve its performance for this type of nonstationary motion. Figure 4.27 presents the time histories of the damping and the tuning ratios of the NSD model during the excitation period.

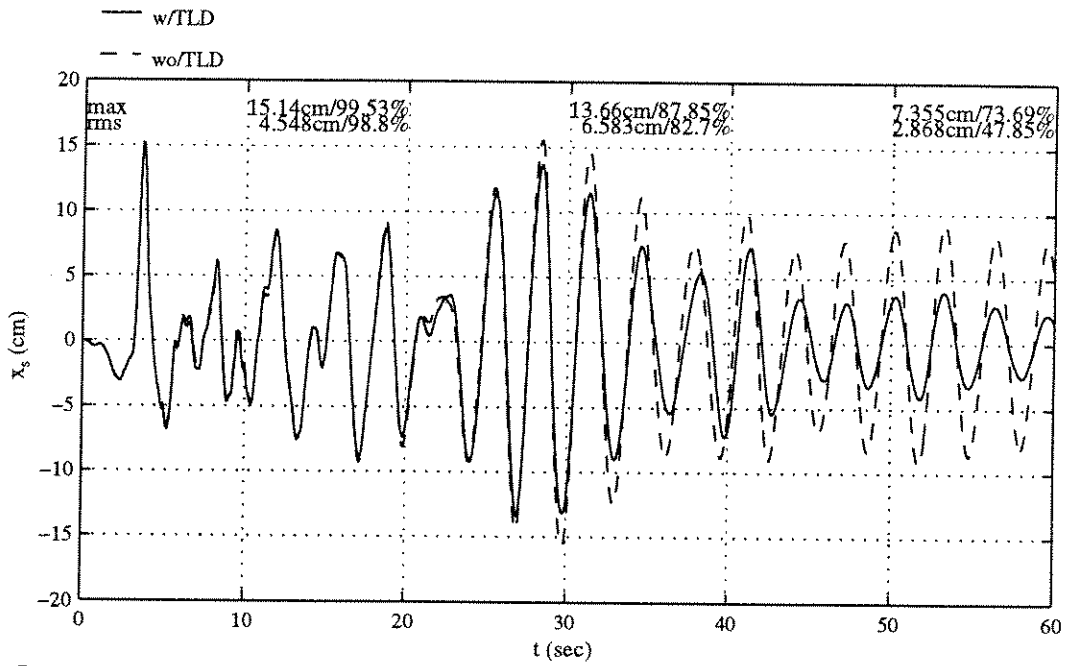

(a) Structural displacement

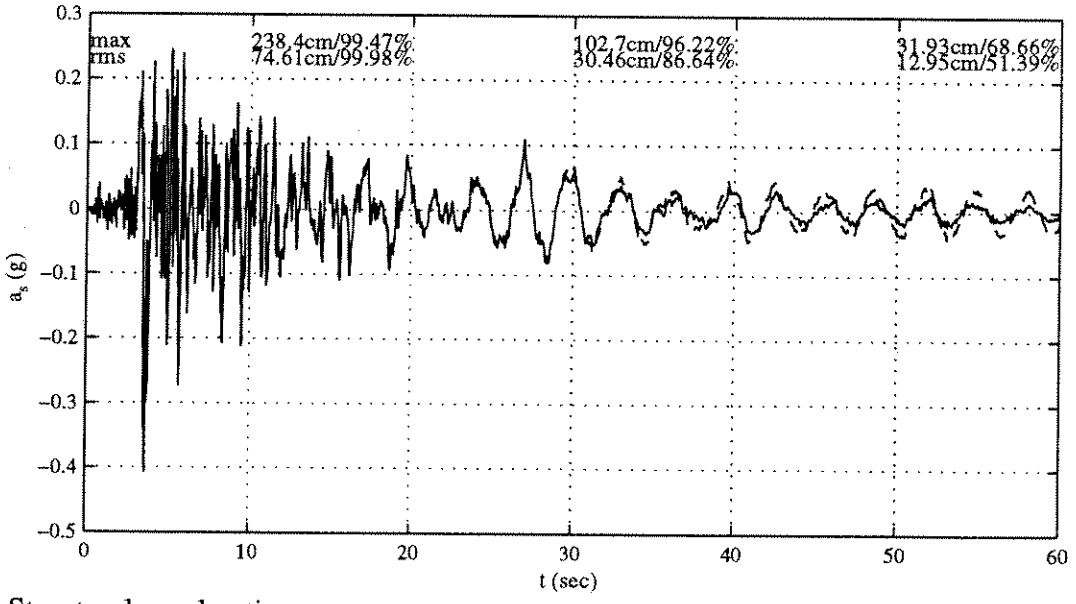

(b) Structural acceleration

Figure 4.26 Time history responses of the structure with and without a TLD under the Northridge earthquake. Structure with f_s = 0.32 Hz and ζ_s = 1.0 %; TLD with L = 171 cm, h_0 = 11.6 cm and μ = 1.0 %.

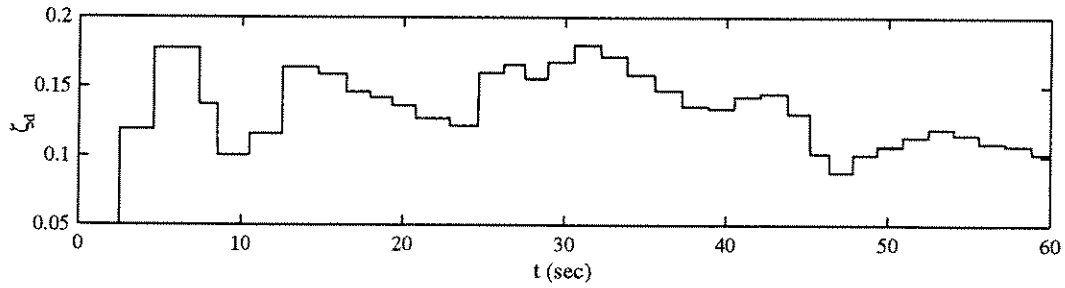

(a) Damping ratio, ζ_d

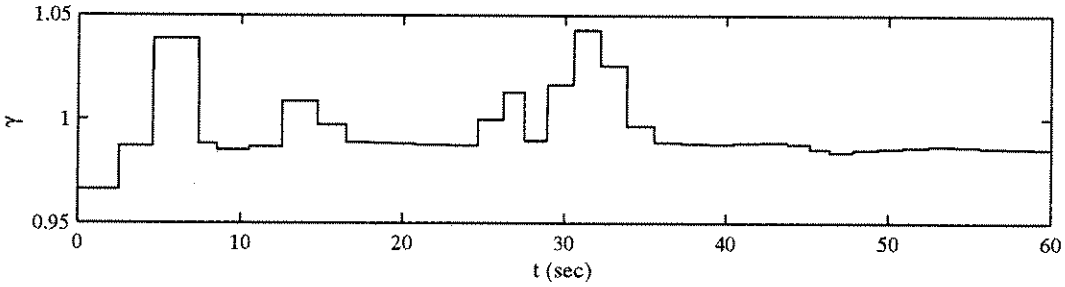

(b) Tuning ratio, γ

Figure 4.27 Time histories for the damping ratio and tuning ratio of the NSD model for the case of Figure 4.26.

CHAPTER 5

CONCLUSIONS

The fundamental behavior of shallow water sloshing motion in TLDs was investigated experimentally and numerically. The results reveal the following:

- Shallow water possesses hardening-spring type nonlinear characteristics. The nonlinearity is dependent upon the excitation amplitude.
- The nonlinearity of the TLD was quantified using the parameter "jump-frequency". The jump-frequency may be explicitly expressed as a function of nondimensional excitation amplitude, $\Lambda = \frac{A}{L}$.
- Regions of weak wave breaking and strong wave breaking were identified. In the region of strong wave breaking, the nonlinear behavior changes more rapidly.
- As the excitation amplitude increases, the frequency range for which the damper is effective widens. This fact indicates that the TLD performs in a wider frequency range under strong excitation, i.e., it is a robust energy-dissipating system.
- Higher frequency components of the water sloshing motion do not influence significantly the energy dissipation capacity of the TLD. An approximate analysis method using only the fundamental mode is valid.
- The damping forces due to water sloshing motion can be adequately calculated based on the hydrostatic pressure assumption at the end walls of the rectangular tank.

An equivalent TMD of the rectangular TLD (NSD model) was developed based upon the shaking table experiments. The damping ratio and the stiffness hardening ratio of the NSD model were explicitly expressed as functions of the parameter (A/L). In the weak wave breaking region, the stiffness of the NSD model changes only slightly and

remains approximately constant at a value of 1.05. In the strong wave breaking region, the stiffness changes rapidly. This phenomenon is consistent with the jump-frequency investigation.

Although the water sloshing motion in a circular tank is more complex than that in the rectangular one, preliminary experimental results suggest it may be treated as an equivalent rectangular tank for design purposes.

A numerical scheme to solve the shallow-water equation using the Random Choice Method (RCM model) proposed by Gardarsson and Yeh (1994) predicts quite accurately the water sloshing motion in the region of weak wave breaking, i.e. $A/L < 0.03$. However, the RCM model cannot simulate accurately the water sloshing with strong wave breaking that occurs in the excitation range $A/L > 0.03$.

Based on the observed nonlinearity of the TLD, nonlinear tuning was proposed. The nonlinearly tuned TLD was shown to perform more effectively than the linearly tuned one.

Numerical solution schemes in the time domain for interaction of the TLD with a SDOF structure were developed. The behavior of the TLD was simulated using the NSD and the RCM models, respectively. These solution schemes were employed to evaluate the TLD performance under various excitation conditions.

Iterative solution procedures for the frequency responses of a SDOF structure equipped with a TLD were proposed for the structure subjected to harmonic or white noise excitations. Using the solution schemes, the parameters of the NSD model may be determined. The effectiveness of the TLD may be estimated using the proposed frequency response method.

The performance of TLDs attached to lightly damped structures was evaluated using the proposed numerical solution schemes for the structure under various excitation conditions (harmonic forcing, white noise forcing, wind or earthquake). The results of extensive numerical investigations reveal the following:

- For harmonic or white noise excitations, the optimization of the parameters for the NSD model follows that of the traditional linear TMD. The nonlinear tuning enhances the performance of the TLD.

- Effectiveness of TLDs was evaluated for a structural system subjected to typical time-varying wind pressure loadings. The wind pressure loading was simulated using an AR(2) model proposed by Reed (1983). These preliminary results from the time-history numerical analyses show that the selected TLDs reduce the RMS structural accelerations up to 40 %. This result illustrates the viability of the NSD model. Further investigation of the TLD performance for time series representation of various wind loadings is warranted.

- The effectiveness of the TLD under earthquake conditions was investigated numerically. Northridge earthquake ground motions were imposed on a lightly damped SDOF structure equipped with a nonlinearly tuned TLD. The TLD does not reduce the structural response during the initial stage of the earthquake. This limitation indicates the inability of this passive system for damping "impact-type" loadings. The performance of the TLD for earthquake loadings must be further investigated.

REFERENCES

Ayorinde, E.O. and Warburton, G. B., 'Minimizing structural vibration with absorbers', Earthquake Engineering and Structural Dynamics. Vol. 8, 219-236, 1980.

Benito, M., Pacheco, M. and Fujino, Y., 'Perturbation Technique to Approximate the Effect of Damping Nonproportionality in Modal Dynamic Analysis', JSCE, Structural Engineering / Earthquake Engineering, Vol. 6, No. 1, 169-178, 1989.

Blevins, R.D., Formulas for Natural Frequency and Mode Shape, Robert E. Krieger Publishing Company, Malaber, Florida, pp. 368.

Chaiseri, P., Fujino, Y., Pacheco, B. M. and Sun, L. M., 'Interaction of Tuned Liquid Damper (TLD) and Structure - Theory, Experimental Verification and Application.' J. Structural Engineering / Earthquake Engineering, Proc. JSCE, Vol. 6, No. 2, 273-282,1989.

Chester, W., 'Resonant Oscillation of Water Waves. I. Theory & II. Experiment.' Proceedings, Royal Society of London, A306, pp.5-39, 1968.

Den Hartog, J. P., 'Two degree of freedom', Mechanical Vibrations, 4th ed, McGraw-Hill, New York, pp. 79-120, 1956.

Faltinson, O.M., 'A Numerical Nonlinear Method of Sloshing in Tanks with Two-Dimensional Flow.' J. of Ship Research, Vol.22, pp.193-202, 1978.

Fediw, A. A., Breukelman, B., Morrish, D. P. and Isyumov, N., 'Effectiveness of a Tuned Sloshing Water Damper to Reduce the Wind-Induced Response of Tall Buildings', Proc. of the 7th U.S. National Conference of Wind Engineering, Vol. 1, Los Angeles, June 27-30, p233-242, 1993.

Fediw, A. A., Isyumov, N. and Vickery, B. J., 'Performance of a One Dimensional Tuned Sloshing Water Damper', to be presented at the 1st IAWE European and African Regional Conference, Guernsey, September, 1993.

Fediw, A. A., Isyumov, N., Morrish, D. P. and Breukelman, B., 'Dynamic Behaviour of a Tall Reinforced Concrete Building', ASCE Structures Congress '92, San Antonio, Texas, April, 1992.

Friberg, P. A. and Susch, C. A., 'A User's Guide to Strongmo: Version 1.0 of NCEER's Strong-Motion Data Access Tool for Pcs and Terminals', Lamont-Doherty Geological Observatory of Columbia University, Palisades, New York, 1990.

Fujii, K., Tamura, Y., Sato, T. and Wakahara, T., 'Wind-Induced Vibration of Tower and Practical Applications of Tuned Sloshing Damper,' J. of Wind Engineering, Japan Association for Wind Engineering, No. 37, pp. 537-546, 1988.

Fujii, K., Tamura, Y., Sato, T. and Wakahara, T., 'Wind-Induced Vibration of Tower and Practical Applications of Tuned Sloshing Damper,' J. of Wind Engineering and Industrial Aerodynamics, 33, 263-272, 1990.

Fujino, Y. and Abe, M., 'Design Formulas for Tuned Mass Dampers Based on a Perturbation Technique', Earthquake Engineering and Structural Dynamics, Vol. 22, 833-854, 1993.

Fujino, Y., et al., 'Tuned Liquid Damper (TLD) for Suppressing Horizontal Motion of Structures', ASCE, J. of Engineering Mechanics, Vol. 118, No. 10, 1992.

Fujino, Y., Pacheco, B. M., Chaiseri, P. and Sun, L. M., 'Parametric Studies on Tuned Liquid Damper (TLD) Using Circular Containers By Free-Oscillation Experiment', J Structural Engineering / Earthquake Eng., JSCE., Vol. 5, No. 2, pp. 381-391, 1988.

Gardarsson, S. and Yeh, H., 'Numerical Simulations of Bores using the Random Choice Method', Proc. the 3rd UJNR Workshop, 1994.

Housner, C.W., 'Dynamic pressure on accelerated fluid containers', Bulletin of the Seismological Society of America, 1959.

Igusa, T. and Der Kiureghian, A., 'Dynamic characterization of two degree of freedom equipment-structure systems', J. Engineering Mechanics, ASCE 111, 1-19, 1985.

Igusa, T. and Xu, K., 'Vibration Reduction Characteristics of Distributed Tuned Mass Dampers', Proc., 4th Intl. Conf., Structural Dynamics: Recent Advances, Southampton, UK, 1991, pp. 596-605.

Igusa, T. and Xu, K., 'Vibration Control using Multiple Tuned Mass Dampers', J. of Sound and Vibration, 175(4), pp. 491-503, 1994.

Kareem, A. and Sun, W. J., 'Stochastic Response of Structures with Fluid-Containing Appendages', J. of Sound and Vibration, Vol. 119, No. 3, 1987.

Kareem, A., 'Acrosswing Response of Buildings', ASCE, J. Structural Division, Vol. 108, No. ST4, 1982.

Kareem, A., 'Mitigation of Wind Induced Motion of Tall Buildings', J. of Wind Engineering and Industrial Aerodynamics, Vol. 11, 1983.

Kareem, A., 'Reduction of Wind Induced Motion Utilizing a Tuned Sloshing Damper', J. of Wind Engineering and Industrial Aerodynamics, Vol. 36, 1990.

Kareem, A., 'Serviceability Issues and Motion Control of Tall Building', Structures Congress 92, ASCE, pp476-479, 1992.

Kareem, A., 'Tuned Liquid Dampers: Past, Present and Future', Proceedings of the Seventh U.S. National Conference on Wind Engineering, 1993.

Kareem, A., 'Wind Induced Response of Buildings: A Serviceability Viewpoint', AISC, Proceedings of the National Engineering Conference, Miami Beach, Florida, 1988.

Keulegan, G.R.L., 'Energy Dissipation in Standing Waves in Rectangular Basins.' J. Fluid Mechanics, Vol. 6, pp.33-50, 1959.

Koh, C. G., Mahatma, S. and Wang, C. M., 'Theoretical and Experimental Studies on Rectangular Liquid Dampers under Arbitrary Excitations', Earthquake Engineering and Structural Dynamics, Vol. 23, 17-31, 1994.

Koh, C. G., Mahatma, S. and Wang, C. M., 'Reduction of Structural Vibrations by Multiple-Mode Liquid Dampers', Earthquake Engineering and Structural Dynamics, 1995.

Lamb, H., Hydrodynamics, 6th edition, pp. 619-621, Cambridge University Press, 1932.

Lee, J., 'Optimal Weight Absorber Designs for Vibrating Structures Exposed to Random Excitations', Earthquake Engineering and Structural Dynamics, Vol. 19, 1209-1218, 1990.

Lepelletier, T. G. and Raichlen, F., 'Nonlinear Oscillations in Rectangular Tanks' J. of Engineering Mechanics, Vol. 114(1), ASCE, pp. 1-23, 1988.

McNamara, R. J., 'Tuned Mass Dampers for Buildings', J. of the Structural Division, ASCE, Vol. 103, pp 1785-1798, 1977.

Miles, J.W., 'Nonlinear Surface Waves in Closed Basins." J. Fluids Mechanics, Vol.75, pp.419-448, 1976.

Modi, V. J. and Welt, F., 'Damping of Wind Induced Oscillations through Liquid Sloshing', J. Wind Engineering and Industrial Aerodynamics, 30, 85-94, 1988.

Modi, V. J. and Welt, F., 'Vibration Control Using Nutation Dampers', Proc. Int. Conf. on Flow Induced Vibrations, England, pp. 369-376, 1987.

Nakayama, T. and Washizu, K., 'The Boundary Element Method Applied to the Analysis of Two-Dimensional Nonlinear Sloshing Problems', International Journal for Numerical Method in Eng., Vol. 17, pp. 1631-1646, 1981.

Nayfeh, A.H. and Mook, D. T., Nonlinear Oscillations, John Wiley & Sons, Inc., pp. 161-257, 1979.

Nayfeh, A.H., Perturbation Methods, Wiley, New York, pp. 110-114, 1973.

Newland, D.E., An Introduction to Random Vibrations, Spectral & Wavelet Analysis, 3rd ed., Longman Scientific & Technical, pp371-372, 1993

Noji, T., Yoshida, H., Tatsumi, E. and Hagiuda, H., 'Study on Vibration Control Damper Utilizing Sloshing of Water', J. of Wind Engineering, Japan Association for Wind Engineering, No. 37, pp. 557-566, 1988.

Okamoto, T. and Kawahara, M., 'Two Dimensional Sloshing Analysis by the Arbitrary Lagrangian-Eulerian Finite Method', JSCE, Structural Engineering / Earthquake Engineering, Vol. 8, No. 4, 207-216, 1992.

Pacheco, B. M. and Fujino, Y., 'Approximate explicit formulas for complex modes of a two-degree-of-freedom (2DOF) system', Struct. Engineering / Earthquake Engineering, JSCE 6(1), 191-200, 1989.

Reed, D.A. and Scanlan, R.H., 'Time Series Analysis of Cooling Tower Wind Loading', ASCE, J. of Structural Engineering, Vol. 109, No. 2, 538-554, 1983.

Reed, D.A., Yeh, H., Yu, J. and Gardarsson, S., 'Experimental Investigation of Tuned Liquid Dampers', Proc. of the ASCE 1996 International Conference on Natural Disaster Reduction, Washington D.C., December, 1996

Reed, D.A., Yeh, H., Yu, J. and Gardarsson, S., 'Performance of Tuned Liquid Dampers for Large Amplitude Excitation', Proc. of the 2nd International Workshop on Structural Control, Hong Kong, December, 1996

Sayar, B. and Baumgarten, J.R., 'Linear and Nonlinear Analysis of Fluid Sloshing Damper.' AIAA J., Vol.20, No.11, pp.1534-1538, 1982.

Shimizu, T. and Hayama, S., 'Nonlinear Response of Sloshing Based on the Shallow Water Wave Theory', JSME International Journal, Vol. 30, No. 263, pp. 806-813, 1987.

Snaebjornsson, J. and Reed, D. A., 'Wind Induced Accelerations of a Building: A Case Study', Engineering Structures, Vol. 13, 1991.

Sun, L. M., 'Semi-Analytical Modeling of Tuned Liquid Damper (TLD) with Emphasis on Damping of Liquid Sloshing', Ph.D. Thesis, The University of Tokyo, September, 1991.

Sun, L. M., Fujino, Y., Chaiseri, P., Pacheco, B. M., 'The Property of Tuned Liquid Dampers using a TMD Analogy' Earthquake Engineering and Structural Dynamics, Vol. 24, pp. 967-976, 1995.

Sun, L. M., Fujino, Y., Pacheco, B. M and Chaiseri, P., 'Modelling of Tuned Liquid Damper (TLD)' Proc. 8th Int. Conf. on Wind Engineering, London, Canada, 12pp, 1991.

Sun, L. M., Fujino, Y., Pacheco, B. M. and Isobe, M., 'Nonlinear Waves and Dynamic Pressures in Rectangular TLD - Simulation and Experimental Verification -', J. Structural Engineering / Earthquake Engineering, JSCE., Vol. 6, No. 2, pp. 251-262, 1989.

Tamura, Y., Fujii, K., Sato, T., Wakahara, T. and Kosugi, M., 'Wind Induced Vibration of Tall Towers and Practical Applications of Tuned Sloshing Damper', Proceedings Vol. 1, Symposium/Workshop on Serviceability of Buildings, U. of Ottawa, Canada, May 1988.

Tamura, Y., Kousaka, R. and Modi, V. J., 'Practical Application of Nutation Damper for Suppressing Wind Induced Vibrations of Airport Towers', Proceedings of Workshop on Serviceability of Buildings, 1988.

Tsai, H. C. and Lin, G. C., 'Optimum Tuned Mass Dampers for Minimizing Steady State Response of Support Excited and Damped Systems', Earthquake Engineering and Structural Dynamics, Vol. 22, 957-973, 1993.

Tsai, T. C., 'Greens Function of Support Excited Structures with Tuned Mass Dampers by a Perturbation Method', Earthquake Engineering and Structural Dynamics, Vol. 22, 975-990, 1993.

Ueda, T., Nakagaki, R. and Koshida, K., 'Suppression of Wind Induced Vibration by Dynamic Dampers in Tower-like Structures', International Symposium for Innovation in Cable Stayed Bridges, Japan, 1991.

Villaverde, R. and Koyama, L. A., 'Damped Resonant Appendages to Increase Inherent Damping in Buildings', Earthquake Engineering and Structural Dynamics, Vol. 22, 491-507, 1993.

Wakahara, T., 'Wind-Induced Response of TLD-Structure Coupled System Considering Nonlinearity of Liquid Motion', Shimizu Tech. Res. Bull, No. 12, March 1993.

Wakahara, T., Ohyama, T. and Fujii, K., 'Suppression of Wind-Induced Vibration of a Tall Building using Tuned Liquid Damper', J. of Wind Engineering and Industrial Aerodynamics, 41-44, 1895-1906, 1992.

Warburton, G. B. and Ayorinde, E.O., 'Optimal absorber parameters for simple systems', Earthquake Engineering and Structural Dynamics. 8, 197-217, 1980.

Warburton, G. B., 'Optimum Absorber Parameters for Minimizing Vibration Response', Earthquake Engineering and Structural Dynamics, Vol. 9, 251-262, 1981.

Warburton, G. B., 'Optimum Absorber Parameters for Various Combinations of Response and Excitation Parameters', Earthquake Engineering and Structural Dynamics, 10, 381-401, 1982.

Welt, F. and Modi, V. J., 'Vibration Damping Through Liquid Sloshing: Part I --- A Nonlinear Analysis, Part II --- Experimental Results', Proc. Diagnostics Vehicle Dynamics and Special Topics, ASME, Design Engineering Division (DE), Vol. 18-5, pp. 149-165, 1989.

Xu, Y. L. and Kwok, K.C.S., 'Semianalytical Method for Parametric Study of Tuned Mass Dampers', ASCE, J. Structural Engineering, Vol. 120, No.3, 1994.

Xu, Y. L., Samali, B. and Kwok, K. C. S., 'Control of Along Wind Response of Structures by Mass and Liquid Dampers', J. Engineering Mechanics, Vol. 118, No. 1, 1992.

Yamaguchi, H and Harnpornchai, N., 'Fundamental Characteristics of Multiple Tuned Mass Dampers for Suppressing Harmonic Forced Oscillations', Earthquake Engineering and Structural Dynamics, Vol. 22, 51-62, 1993.

Yang, J. N. and Samali, B., 'Control of Tall Buildings in Along Wind Motion', J. Structural Engineering, Vol. 109, No. 1, 1983.